Stony Brook University

Electrospun Mixed Oxide Photocatalysts to Decompose Dyes in Water

A Thesis Presented

by

Sherlyn Divya

to

The Graduate School

in Partial Fulfillment of the

Requirements

for the Degree of

Master of Science

in

Materials Science and Engineering

Stony Brook University

August 2013

Stony Brook University

The Graduate School

Sherlyn Divya

We, the thesis committee for the above candidate for the

Master of Science degree, hereby recommend

acceptance of this thesis.

Perena Gouma
Professor Department of Materials Science and Engineering

T.A. Venkatesh
Assistant Professor Department of Materials Science and Engineering

Gary Halada
Associate Professor Department of Materials Science and Engineering

This thesis is accepted by the Graduate School

Charles Taber
Interim Dean of the Graduate School

Abstract of the Thesis

ELECTROSPUN MIXED OXIDE PHOTOCATALYSTS TO DECOMPOSE DYES IN WATER

by

Sherlyn Divya

Master of Science

in

Materials Science and Engineering

Stony Brook University

2013

In this work, four catalysts have been studied for their photocatalytic efficiency by testing each with methylene blue dye solution. Three catalysts were synthesized by the electrospinning method and then compared with the fourth commercially available catalyst for their photocatalytic activity.

The basic metal oxide studied was titanium dioxide. Nanocomposite mats of pure titania, copper doped titania and copper doped degussa P25 titania, were synthesized using the electrospinning method. The pure titania and copper doped titania nanocomposites possessed the anatase phase which was obtained by annealing the as-spun nanocomposites at 450^0C. All the catalysts were analyzed for their photocatalytic activity both under ultra-violet light and under visible light. The aim of this work was to synthesize titania photocatalysts, demonstrate their photocatalytic activity with methylene blue solution under UV-light and visible light and

compare their activities with the commercial titanium dioxide (degussa P25). It is important to synthesize visible light active photocatalysts as these could be activated under a wide spectrum of natural sunlight unlike the degussa titanium dioxide. Doping was incorporated in order to narrow the band gap energy of the photocatalyst for achieving higher efficiency especially under visible light irradiation.

The morphology and size of the synthesized photocatalysts were studied by characterizing them with Scanning Electron Microscopy, Energy Dispersive X-Ray Spectroscopy, Transmission Electron Microscopy and X-Ray Diffraction. The photocatalytic activity tests were carried out using UV-Vis Spectroscopy. It was found that the electrospun pure titania and copper doped titania fibers were activated under the visible light spectrum unlike the degussa titanium dioxide. The copper doped titania provided to be the most efficient photocatalyst under visible light radiation and the importance of this finding can be extended for treating industrial wastewaters by just exposing it to natural sunlight in the presence of this photocatalyst.

Dedication Page

Dedicated to my Parents.

Table of Contents

List of Figures

List of Tables

Acknowledgments

I am sincerely grateful to my Professor Perena Gouma for giving me an opportunity and showing faith in my ability to work on this project. She has always encouraged ideas and suggestions from me. In spite of her busy professional schedule, she has done her best to make time to discuss all my issues and guide me in the right path of my research. She has been a constant support throughout my thesis work, making me feel comfortable when I was a beginner and always welcomed with me a big smile! I am very thankful to her for providing me with funding through the NSF grant.

I thank Professor T.A. Venkatesh and Professor Gary Halada for accepting my request to be on the committee panel of this thesis and for their time and patience in reviewing my work.

A special thank you to my labmate Jusang Lee for helping me at all times during my experiments, for all his advice that helped me in my work and also for being a friendly labmate. I would also like to thank Gagan Jodhani and Shanthanu Sood for their support. I thank Jim Quinn for assisting me with the SEM instrument whose results are an important part of my thesis.

I would like to extend my gratitude to my parents for being my strength and support throughout my research. I would like to thank my friend Sumantu Iyer in a very special way for he constantly pushed me to work hard, advised me throughout the year of my research, and comforted me during my bad times.

Above all, I thank God for all his blessings showered upon me without which this would have not been possible!

CHAPTER 1: INTRODUCTION

Water is precious, valuable and essential to all life on this planet. Even though 71% of the earth is covered with water, only 1% is fresh, usable water. The growth of population in the world has increased the demand for water. Today with the numerous industries, the demand for water supply is increasing. In fact in developed countries, the industrial sector is blamed to be using 50 to 80 percent of the total demand for water. In spite of consuming a huge percent of water, the industries also produce very large amounts of wastewater which is disposed into near-by rivers, constituting high water pollution. The color of water is a result of a natural (humic substance) or artificial (disposal of dyes as effluent) phenomenon (Dos Santos et al., 2007). Colored wastes block out the penetration of light into the waters and thus cause a negative effect on the underwater lives since light plays an important role in balancing the ecosystem of aquatic life.

Among all the industries, the textile industry is said to be consuming the most amount of water for its processing, that include pre-treatment, dying, printing and finishing(Allegre, Moulin et al. 2006). For instance, in a typical dying process, the harmful colored wastes come from the water vapor that is used to heat the dye baths and from the liquid water that is used to ensure transmission of the dye onto fibers. Once the process is complete, the industry discharges its highly toxic and heavily dyed wastes into the rivers which accounts for water pollution. Since it is almost impossible to estimate the total amount of pollutants released each time by these industries, this calls for expensive methods to clean the waters and make it useful for drinking. Public concerns have been on a high because of this critical state of the waters and governments have placed strict laws for the same (Perciasepe, McLerran et al. 2013). This problem has since then been a challenge for researchers working in the developing fields of water treatment, encouraging them to come up with the best methods to minimize the wastes and purify water.

Semiconductor photocatalysis has been a promising area of research in the recent years, for it has shown great potential in contributing to environmental pollution. Semiconductor materials such as TiO_2, ZnO, SnO_2, GaP, SiC, CdS and Fe_2O_3 (Sayilkan, Asilturk et al. 2007) have been used in the photocatalytic oxidation of organic compounds. TiO_2, ZnO and SnO_2 have extensively been used for the removal of organic contaminants (Sakthivel, Neppolian et al. 2003, Irmak, Kusvuran et al. 2004, Akyol and Bayramoglu 2010). Among all of these, TiO_2 is said to be the semiconductor photocatalyst which is most widely used since it is highly active, non-toxic, cost effective, less water soluble, of good chemical stability and has environment friendly characteristics (Thiruvenkatachari, Kwon et al. 2007, Tseng, Lin et al. 2010). Fujishima and Honda in 1972, discovered the photocatalytic activity of TiO_2 (Song, Wu et al. 2007, Leary and Westwood 2011).

1.1 Photocatalysis

Photocatalysis is aptly explained as the acceleration of a photoreaction by the presence of a catalyst. As reported by many scientists, photocatalytic reactions occur by absorbing a photon of energy that is equal to or greater than the band gap energy of the semiconductor. Band gap energy is the difference in energy between the valence and the conduction band. Photoinduced transfer of electrons occurring in adsorbed species on semiconductor photocatalyst, is said to be dependent on the band positions of the semiconductor in use and also its redox potentials(Fujishima, Rao et al. 2000) . Figure 1 shows the valence and conduction band energy diagrams for some semiconductors:

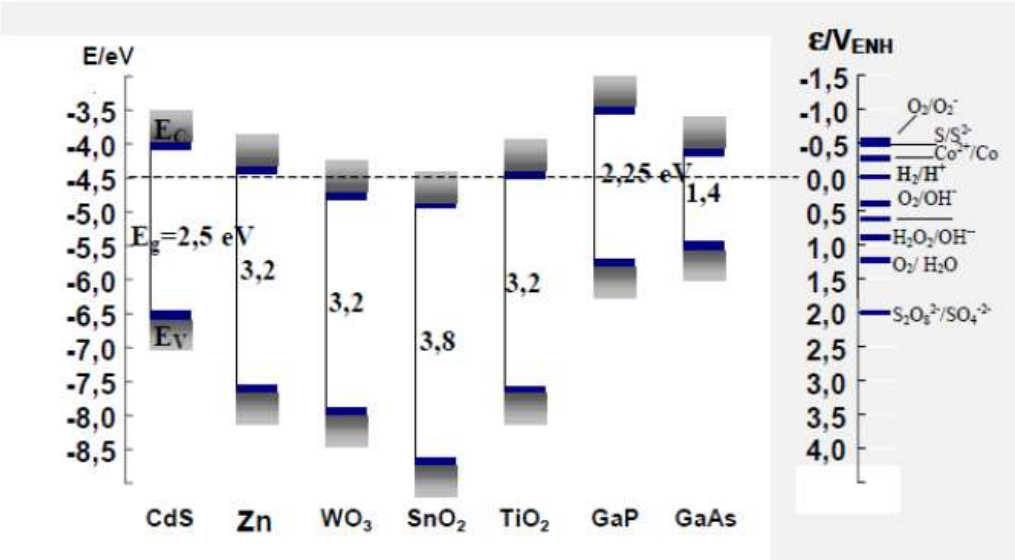

Figure 1: Diagram of valence and conduction bands for different semiconductors (Colmenares, Luque et al. 2009)

The table 1 below shows the band gap energies for some semiconductors in decreasing order of energy:

Table 1: Band gap energies of semiconductors

Semiconductor	**Band gap Energy (eV)**
SnO_2	3.5
ZnO	3.2
TiO_2 (anatase)	3.2
TiO_2 (rutile)	3.0
WO_3	2.8
CdS	2.5
Fe_2O_3	2.3
Si	1.1

A photocatalytic reaction is initiated when an excited atom hit by a photon, causes electrons (e^-) to leave their filled valence band, creating holes(h^+), and jumping to the empty conduction band(Childs and Hagar 1980, Pelizzetti, Minero et al. 1989, Tang, Zhang et al. 1997, Sauer, Neto et al. 2002). The photoexcited electron, jumps to the conduction band as the absorbed photon energy ($h\upsilon$) is greater than or equal to the band gap of the semiconductor photocatalyst. It also ends up in generating electron hole pairs ($e^- - h^+$). The following chain reactions have been accepted and used widely (Colmenares, Luque et al. 2009) :

Photoexcitation: $TiO_2 + h\upsilon \rightarrow e^- + h^+$ (1)

Oxygen ionosorption: $(O_2)_{ads} + e^- \rightarrow O_2\bullet^-$ (2)

Ionization of water: $H_2O \rightarrow OH^- + H^+$ (3)

Protonation of superoxides: $O_2\bullet^- + H^+ \rightarrow HOO\bullet$ (4)

Like the scavenging property of O_2 which is formed in the protonation reaction above, the hydroperoxyl radical formed in the same reaction also scavenges and thus this leads to a double prolonged lifetime for the photohole:

$$HOO\bullet + e^- \rightarrow HOO^- \quad (5)$$

$$HOO^- + H^+ \rightarrow H_2O_2 \quad (6)$$

As shown in figure 2, oxidation and reduction reactions can take place at the surface of the semiconductor photocatalyst. When there is available oxygen, recombination of the electron and hole occurs. The oxygen combines with the electrons to form superoxides ($O_2\bullet^-$). These then protonate with the ionized water and form hydroperoxide radical (HOO•) as in equation 4. This radical then interacts with electrons and ionized water (H^+) to finally give H_2O_2.

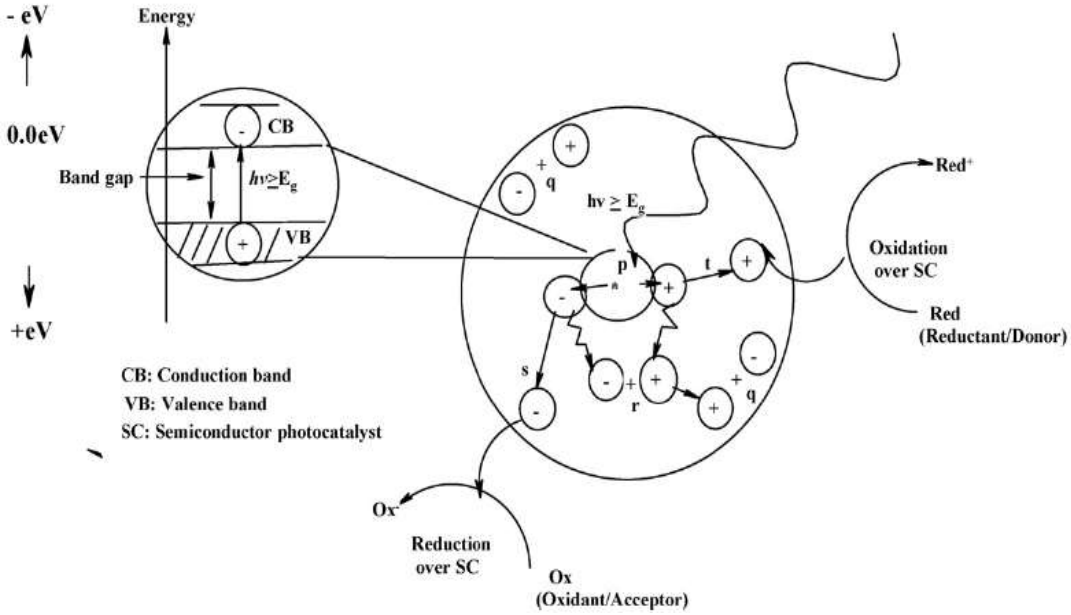

Figure 2: Schematic of the processes in a semiconductor photocatalyst that is excited by a photon: (p) photogeneration of electron/hole pair, (q) surface recombination, (r) recombination in the bulk, (s) diffusion of acceptor and reduction on the surface of SC, and (t) oxidation of donor on the surface of SC particle. Source: (Gaya and Abdullah 2008)

In the photocatalytic process, holes at the surface of the catalyst remove electrons from organic contaminate or take away electrons from hydroxyl nucleophiles, creating hydroxyl radicals. These hydroxyl radicals, then break down the organics and this process is known as AOP (Advanced Oxidation Process). AOPs are very essential reactions in photocatalysis and among the various AOPs, photocatalysis stands as a combination of photochemistry and catalysis. During an AOP process they generate reactive ions which oxidize most contaminants quickly and unselectively (Konstantinou and Albanis 2004). Optimum photocatalytic degradation will be achieved when all the organic contaminants have been completely degraded. This leads to complete mineralization of the organics to water, carbon dioxide, inorganic ions and mineral acid (Sakthivel, Neppolian et al. 2003). Many purifying methods use the photocatalytic technique to destroy contaminants. For example, photocatalysis is used in removing Nitrogen Oxides from air streams that are contaminated(Matsuda, Hatano et al. 2001), to oxidize amino acids in water(Muszkat, Feigelson et al. 2002), treating wastewater that is

contaminated with complex metal and organic chemicals(Prairie, Evans et al. 1993), cleaning coffee stains by a self-cleaning photocatalytic oxidation method (Heller 1995) and many more industrial and commercial uses.

Most of the current research work which use TiO_2 semiconductors, report a band gap for the anatase phase as 3.2eV (Hufschmidt, Liu et al. 2004, Lee, McIntyre et al. 2004) at wavelength of 385nm. Titanium Dioxide is commercially available or also prepared in laboratories. In this research, we have prepared TiO_2 from Titanium Tetra Isopropanol by a sol-gel method, followed by electrospinning and thereby annealing the as-spun fibers. The fibers were then tested for their catalytic activity. TiO_2 being white in color, shows no absorption under the whole spectrum that is including the visible range (Hashimoto, Irie et al. 2005).

1.2 Factors influencing photocatalyst efficiency

There are many parameters which affect the efficiency of a photocatalyst and these are detailed below:

Nature of the photocatalyst:

It has been reported that the rate of a reaction is directly affected by the number of photons hitting a photocatalyst (Kogo, Yoneyama et al. 1980). This implies that reactions occur only on adsorbed sites of the semiconductor photocatalyst. Surface morphologies such as agglomerate size, particle or nanofiber size of nanomaterials play an important role in photocatalytic oxidation processes (Ding, Sun et al. 2005). Synthesis methods have been developed and modified so as to meet requirements for its application (Diebold 2003, Mohammadi, Cordero-Cabrera et al. 2006). For example, nano sized particles of titania have been synthesized for photomineralization of organic compounds since it has been reported to have high activities at a nanometer level (Maira, Yeung et al. 2001).

Quantity of the photocatalyst:

There is always a change in efficiency of a catalyst as the catalyst loading changes. We normally encounter an increase in photocatalytic activity as the concentration of the catalyst increases (Krysa, Keppert et al. 2004). However, there is an optimum level after which the activity of a catalyst is hindered. This is because by adding excess catalyst, there is a reduction in penetration of light into the solution, leading to unfavorable light scattering (Chun, Yizhong et al. 2000). Hence it is important to avoid adding excess catalyst and ensuring that all the efficient photons are totally absorbed(Saquib and Muneer 2003).

Concentration of the substrate:

The concentration of organic substrate over time, depends on the photonic efficiency during oxidation of the photocatalyst (Friesen, Morello et al. 2000). When there is a high concentration of substrates, it is observed that the photonic efficiency decreases, and the surface of titania becomes saturated leading to catalyst deactivation (Arana, Martınez Nieto et al. 2004).

Nature of the substrate:

It is shown that molecules with electron withdrawing groups have shown to adsorb in the dark to a greater extent than electron donating groups (Palmisano, Addamo et al. 2007). Organic molecules that can adsorb to the surface of the photocatalyst have been said to be more inclined to direct oxidation (Tariq, Faisal et al. 2007). Hence, photocatalytic degradation of aromatics depends on the substituent group. It has been reported that nitrophenol has a much stronger adsorbing nature that phenol and therefore degrades faster (Bhatkhande, Kamble et al. 2004).

Intensity of Light:

The efficiency of a photocatalyst largely depends on the radiation absorption of the catalyst (Curco, Gimenez et al. 2002, Ustinovich, Shchukin et al. 2005). It has been reported recently, that there an increase in degradation rate with an increase in the intensity of light (Karunakaran and Senthilvelan 2005, Qamar, Muneer et al. 2006). It has also been shown that the nature or form of light does not affect the reaction rate or degradation rate (Stylidi, Kondarides et al. 2004).

pH level:

The pH of a solution is an influential parameter as it controls the surface charge properties of photocatalysts and size of agglomerates that are formed in a photocatalytic reaction taking place on particulate surfaces (Haque and Muneer 2007). The surface of titanium dioxide could be protonated under acidic conditions or deprotonated under alkaline conditions according to the following equation (Colmenares, Luque et al. 2009):

$TiOH + H^+ \rightarrow TiOH_2^+$ ----- Protonation

$TiOH + OH^- \rightarrow TiO^- + H_2O$ ----- Deprotonation

It has been reported that degussa P-25, has a pzc (point of zero charge- it describes the condition when the electrical charge density on the surface is zero) of 6.9 (Kosmulski 2004). Thus, a titania surface will in an acidic medium i.e. pH<6.9 stays positively charged and remains negatively charged in alkaline medium that is having pH>6.9.

It has been shown that when the pH changes, it leads to enhancement of the photo-removal efficiency of organic pollutants in the presence of titania , without any alteration in reaction rate (Shourong, Qingguo et al. 1997). Research has shown the enhanced degradation of such organic pollutants under optimum conditions (Mansilla, Bravo et al. 2006).

Temperature:

The influence of reaction rate with temperature, on the photocatalytic activity of a catalyst has been discussed by many researchers since a very long time. There have been reports proving the dependence of reaction rate on the temperature of a reaction. It shows that as the temperature of the reaction increases, the photocatalytic activity decreases. This is because when the reaction temperature increases, it tends to enhance the recombination of electron-holes, and also enhances desorption of adsorbed species from the surface of the catalyst. These results also seem to be in agreement with the Arrhenius equation in which first order rate constant increases with exp(-1/T).

All these factors contribute to the efficiency of a photocatalyst. Demonstrations on how the catalyst efficiency changes by varying each factor has not been done in this work since the focus of this study was to achieve a better catalyst by doping and comparing the various catalysts to degussa TiO_2. Thus certain values for each factor has been chosen by referring previous

experimental studies that demonstrated the optimum values for each. Therefore, a nano meter range of 100-400nm, a methylene blue organic substrate, a 50ppm concentration of substrate, 0.018g of catalyst, pH level of 7, room temperature and a light intensity of 25mW/cm^2 was used in this work according to literature to achieve an effective photocatalyst (Lakshmi, Renganathan et al. 1995, Xu, Shi et al. 1999, Ling, Mohamed et al. 2004, Yan, Ohno et al. 2006, Xiao, Zhang et al. 2008).

1.3 Mechanism of TiO_2 photocatalysis

Titanium dioxide has been used widely as a photocatalyst because of its nature of generating charge carriers. These carriers induce oxidation and reduction processes(Kim, Lee et al. 2005). In most cases, ΔG is has a negative value for aerobic titania assisted photocatalytic reactions contrary to a photosynthetic reaction (Carp, Huisman et al. 2004). The complementary acid HA of the non-metallic substituent is formed as a by-product (Gaya and Abdullah 2008):

$$\text{Organic wastes} \xrightarrow{TiO_2/O_2/\ h\upsilon \geq Eg} \text{Intermediate(s)} \longrightarrow CO_2 + H_2O + HA \qquad (7)$$

[>$Ti^{IV}OH^{\bullet+}$] represents the surface trapped valence band electrons and [>$Ti^{III}OH$] represents the surface trapped conduction band electrons. Since [>$Ti^{IV}OH^{\bullet+}$] is chemically equivalent to the surface trapped holes, these could be used interchangeably (Lawless, Serpone et al. 1991) and could be said to be indistinguishable species. There exists a good relationship between the surface charge carriers, their surface densities and the efficiency of the TiO_2 photocatalyst. According to Colombo and Bowman (Colombo and Bowman 1996), who conducted a spectroscopic study on TiO_2, the hole-transfer reaction can successfully compete with pico-second electron-hole recombination for species that are adsorbed onto TiO_2. The following reactions have been shown below and described in Figure 3:

Photoexcitation: $TiO_2 + h\upsilon \rightarrow e^-_{CB} + h^+_{VB}$ (8)

Charge carrier trapping: $e^-_{CB} \rightarrow e^-_{TR}$ (9)

Charge carrier trapping: $h^+_{VB} \rightarrow h^+_{TR}$ (10)

Electron-hole recombination: $e^-_{TR} + h^+_{VB}\ (h^+_{TR}) \rightarrow e^-_{CB} + \text{heat}$ (11)

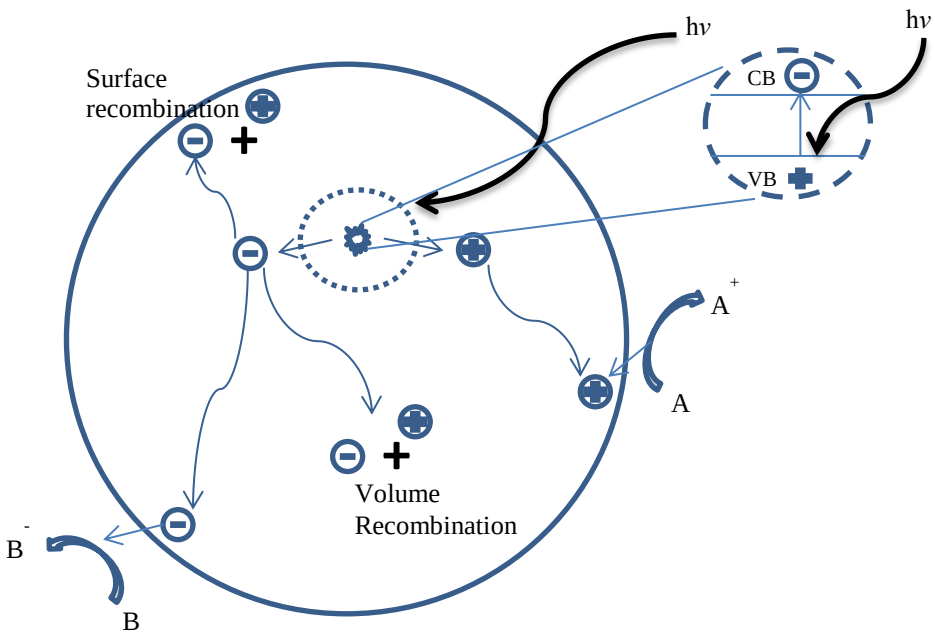

Figure 3: Photocatalytic process over a TiO_2 semiconductor

The ultimate aim of these photocatalytic processes, are to have reactions between an oxidant and an activated electron to produce a reduced product and to have reactions between a reductant and generated holes to produce an oxidized product, while minimizing the recombination of holes. During the process, electrons that are generated could either reduce the dye or react with electron acceptors adsorbed on the surface of Ti(III) or that are dissolved in water, thereby forming superoxide radical anion $O_2^{-\bullet}$ (Konstantinou and Albanis 2004). The photogenerated holes can oxidize the organic compound to form R^+ or react with OH^-/H_2O to form $OH^\bullet$ radicals. So together with some very reactive oxidants, they have said to be responsible for the heterogeneous TiO_2 photocatalytic degradation of organics like dyes. The final $OH^\bullet$ radical that is a very strong oxidizing agent, could oxidize most azo dyes rendering them into mineral end products. The relevant reactions according to this, occurring at the surface of the semiconductor photocatalyst, can be shown as follows (Konstantinou and Albanis 2004):

$TiO_2 + hv(UV) \rightarrow TiO_2\ (e^-_{CB} + h^+_{VB})$ (12)

$TiO_2 (h^+_{VB}) + H_2O \rightarrow TiO_2 + H^+ + OH^\bullet$ (13)

$TiO_2 (h^+_{VB}) + OH^- \rightarrow TiO_2 + OH^\bullet$ (14)

$TiO_2 (e^-_{CB}) + O_2 \rightarrow TiO_2 + O_2^{-\bullet}$ (15)

$O_2^{-\bullet} + H^+ \rightarrow HO_2^\bullet$ (16)

Dye + $OH^\bullet \rightarrow$ degradation products (17)

Dye + $h^+_{VB} \rightarrow$ oxidation products (18)

Dye + $e^-_{CB} \rightarrow$ reduction products (19)

Where hv is the energy of the incident light the photon energy which excites the electron.

1.4 Titania versus other photocatalysts

Although there are numerous number of photocatalysts available which include metal oxides, zeolites, metal chalcogenides and many more, Titanium Dioxide has been the most widely used photocatalyst since many years. The reason is that Titania almost acts as an ideal photocatalyst having the following attributes which make it one of the best (Carp, Huisman et al. 2004):

- Photo-stability even in water
- Inert nature (chemically and biologically)
- Cost effective
- Ability to react with water to generate hydroxyl ions on absorbing light, due to its band gap position

TiO_2 exists in three phases and they are anatase, rutile and brookite. Since brookite is unstable above temperatures of 150^{o}C, the most commonly used phases in photocatalysis are anatase and rutile. The Figure 4 below shows an anatase crystal structure and a rutile crystal structure.

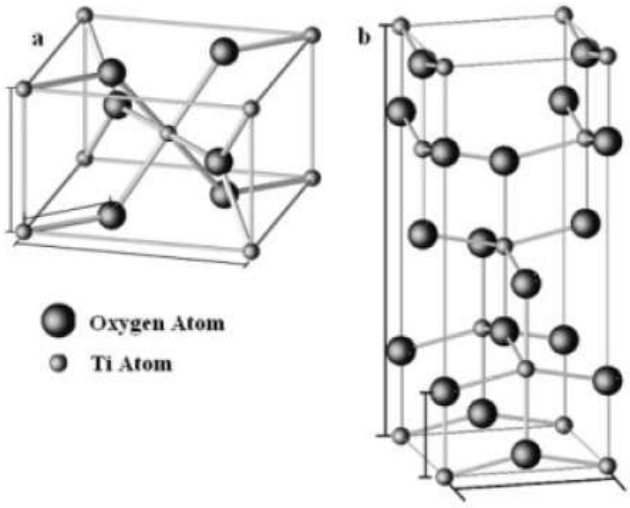

Figure 4: Crystal structures of TiO_2 : (a) rutile unit cell (b) anatase unit cell Source : (Banerjee 2011)

The anatase structure of TiO_2 has some free electrons in its crystal structure and so it happens to be n type semiconductor. It has also been reported that the anatase form provides the best combination of photoactivity and photostability (Colmenares, Luque et al. 2009, Park, Lee et al. 2009). The anatase (band gap 3.2eV) and rutile (band gap 3.0eV) structures however absorb only in the UV region of the entire spectrum. Rutile phase still works for wavelengths closer to the visible region. Photocatalysis with TiO_2 works in the wavelength range of 300-388nm, while the anatase is said to be active at a wavelength corresponding to 388nm (Colmenares, Luque et al. 2009). The solar radiations contain not only UV rays (10nm-400nm) but also made up of visible (400-800nm) and infrared rays (700nm-1mm) and so it becomes hard to get TiO_2 to work efficiently under solar light due to its band gap that is activated upon wavelengths of the UV range only. This lack of photocatalytic activity of TiO_2 under visible light, causes severe limitations for its use (Kisch and Macyk 2002, Yamashita, Takeuchi et al. 2004, Kitano, Matsuoka et al. 2007). The reason behind its inactivity is that the anatase phase of titania has a large band gap i.e. 3.2eV, which corresponds to the start of the absorption band at about 350nm. This onset of the absorption band is not adequate to bring about efficient solar activity since only 5% of the solar radiation is actually absorbed by TiO_2 semiconductor(Colmenares, Luque et al. 2009).

1.5 Modified TiO_2 for visible light photocatalysis

In the past, researchers have developed two strategies to bring about visible light photocatalysis using TiO_2 as a photocatalyst. The first one is by incorporating an organic dye as a photosensitizer and the second is by doping TiO_2 with metallic/non-metallic elements (Pichat, Guillard et al. 1993, Choi, Termin et al. 1994, Abe, Sayama et al. 2004, Yamashita, Takeuchi et al. 2004, Bacsa, Kiwi et al. 2005, Colmenares, Aramendia et al. 2006, Jin, Zhang et al. 2006, Rengaraj and Li 2006, Chen, Huang et al. 2007, Jin, Zhang et al. 2007)

In the first strategy, the degradation of the dye is minimized by a quenching process of the dye's oxidation state with a suitable electrolyte, all done under no air or oxygen conditions.(Pichat, Guillard et al. 1993, He, Zhao et al. 1997, Bauer, Boschloo et al. 2002, Abe, Sayama et al. 2004, Jin, Zhang et al. 2006, Jin, Zhang et al. 2007)

The second strategy, has utilized metallic or non-metallic elements to dope titania and make it responsive in the visible range (Karakitsou and Verykios 1993, Pichat, Guillard et al. 1993, Abe, Sayama et al. 2004, Yamashita, Takeuchi et al. 2004, Bacsa, Kiwi et al. 2005, Jin, Zhang et al. 2006, Jin, Zhang et al. 2007). This doping introduces either occupied orbitals (which leads to negative doping) or unoccupied orbitals (which leads to positive doping) in the band gap area of the semiconductor, thereby reducing the band gap.

In the past, Titania has been doped with various metals like Pt, Au, V, Cr, Mn, Cu, Fe and Ni causing a large shift in its absorbance band, moving into the visible region. For example, titania photocatalyst has shown to be more efficient by doping with noble metals like Pt nanoparticles (Kudo and Miseki 2009). Although there has been a shift in absorbance, there have been controversies on an increase and a decrease in photo-catalytic activity on metal doping that has been reported (Ge and Xu 2006, Lin, Tseng et al. 2006, Aramendia, Colmenares et al. 2007, Kryukova, Zenkovets et al. 2007). These controversies mainly stem from the doping procedures and the undefined nature of the final material. In most cases, the controversies arise from the way in which the metal has been introduced into the material and also the concentration of the metal (dopant). Thus it has been observed that there is an optimal value or level for doping TiO_2 which

in many cases is between 3-7 at.wt% to reach maximum efficiency and any increase from that level would cause a decrease in the photocatalytic activity of the catalyst (Fu, Vary et al. 2005, Okato, Sakano et al. 2005, Chen, Huang et al. 2007, Bensaha and Bensouyad 2012).

1.6 Doping with copper

Although doping with nobel metals like Pt, have attracted great attention and been very promising to photooxidation activities, its high cost and indefinite sustainability, have made researchers look for other dopants that would be an ideal pick for long term solutions (Chong, Jin et al. 2010). Transition metals like Copper are available at low costs and seem to be a good choice in employing it as a dopant with TiO_2 to increase its photocatalytic activity. There have been few investigations done on the doping of copper with titania (Tseng, Wu et al. 2004, Park, Kim et al. 2006, Xu, Liang et al. 2008) resulting in enhanced photocatalytic activity, hydrogen generation (Teleki, Bjelobrk et al. 2008) and carbon dioxide reduction (Sakata, Yamamoto et al. 1998, Li, Wang et al. 2010)

1.7 Methods for doping

Over the past several years, lot of research had been done on using TiO_2 and modified forms of TiO_2 as photocatalysts in the degradation of industrial pollutants like dyes. To list a few in 2001 Gong et al. synthesized porous titanium dioxide nanotubes by the anodic oxidation process, which had tubes that ranged from 25nm to 60nm in diameter, having a morphology that was open at the top and closed at the bottom. This served important applications in biomedical and catalytic areas (Gong, Grimes et al. 2001). Das et al. fabricated nanotubes of TiO_2 by the anodization process and after they studied the cell-material interaction, it was concluded that these nanotubes served better in the medical field than polished Ti-controlled surface (Das, Bose et al. 2009). Kanjwal et al. fabricated TiO_2 photocatalysts with silver nanoparticles and achieved a strong degradation (Kanjwal, Barakat et al. 2010). Li et al. prepared porous TiO_2 nanofibers by

an alkali-dissolution method which increased the surface to volume ratio, and thus the efficiency of the photocatalyst (Li, Sun et al. 2011). Slimen et al. used sol-gel method to prepare TiO_2 activated carbon composites which showed better dye degradation than the degussa P25 titanium oxide (Slimen, Houas et al. 2011). It was shown by Meng and others, that synthesizing TiO_2 nanorods on the surface of TiO_2 nanofibers exhibits better photocatalytic activity than just pure TiO_2 nanofibers (Meng, Shin et al. 2011). All these above mentioned techniques showed a pathway to a good photocatalyst. However, there was complexity involved in all of these preparation techniques and most had high costs of production.

Helaili et al. in 2009 have shown that a modification to the optical property of TiO_2 was brought about by the Copper doped TiO_2 nanoparticles, and this has caused the composite material to show activity in the visible region of solar radiations, thus ultimately enhancing the degradation of organic pollutants (Helaili, Bessekhouad et al. 2009). However, the photocatalytic nanoparticles combine to form aggregates which become attractive sites for the photogenerated electrons and holes, leading to recombination reactions which hinders photocatalysis (Choi, Kim et al. 2010). Aggregates of nanoparticles also have a negative effect on the reusability aspect of a photocatalyst (Pan, Dou et al. 2010). Considering these effects of nanoparticles, research has advanced and synthesized nanotubes of CuO which had TiO_2 nanoparticles decorated on it which was shown to be exhibiting a highly active photocatalysts to decolorize methylene orange dye (Wu, Zhu et al. 2011). Nevertheless, it was noticed that this morphology of the TiO_2 nanoparticles on the CuO nanotube did not serve well for dye degradation, as the nanoparticles of TiO_2 occupied significant surface area of the CuO nanotubes, as well as formed agglomerates which resulted in low surface area of the nanotube for dye adsorption (Wu, Zhu et al. 2011). The agglomeration does not seem to benefit in any way, as it also causes a less uniform structure, decreasing the contact between CuO nanotubes and TiO_2 nanoparticle (Wu, Zhu et al. 2011). Hence, it has been a challenge to eliminate this phenomenon of agglomeration.

To eliminate all of the above mentioned difficulties, photocatalysts were designed to have nanofibrous morphology which was achieved by an electrospinning processing method. The key features of the synthesized photocatalysts were: nanofibers for high surface area, anatase phase of titania for better photocatalytic activity, copper doping to reduce the band gap and electrospinning processing method to eliminate agglomeration and produce fibrous mats.

1.8 Electrospinning

Electrospinning was first observed in 1897 by Rayleigh, studied in detail by Zeleny in 1914 (Zeleny 1914) and patented by Formhals in 1934. Taylor in 1969, laid the groundwork for electrospinning by his work on the electrically driven jets in the electrospinning process (Taylor 1969). The electrospinning technique seems to have regained its importance in the 1980's at a time when nanotechnology was a field of immense interest for scientists. By using the electrospinning process it was possible to fabricate ultrathin fibers that ranged from a few microns to nanometers (Huang, Zhang et al. 2003) thus finding applications in nanotechnology.

The Process:

The electrospinning process is a unique process of spinning, where electrostatic forces produced from a high voltage supply, are applied to a polymer solution, forming jets that lead to ultrafine fibers. These fibers have diameters that are a few micrometers to nanometers in size, and a very large surface area, thus making it a better technique than conventional spinning methods that are based on melt and solution spinning. Due to the high surface area of fibers which are in the submicron scale, these fibers find numerous applications ranging from composites, sensor materials, catalysts, filtration to tissue scaffolds. Many other processes like the pesticide sprayers and electrostatic precipitators have a similar working principle to the electrospinning process. These are based on strong mutual charge repulsions that overcome weaker forces of surface tension in a polymer solution (Chew, Wen et al. 2006).

With the expansion of the electrospinning technique, researchers have designed and developed well refined techniques that electrospin complex fibrous structures efficiently (Kidoaki, Kwon et al. 2005, Stankus, Guan et al. 2006). However, there are two standard methods or setups for electrospinning: Vertical Setup as shown in Figure 5(a) and the Horizontal Setup as shown in Figure 5(b).

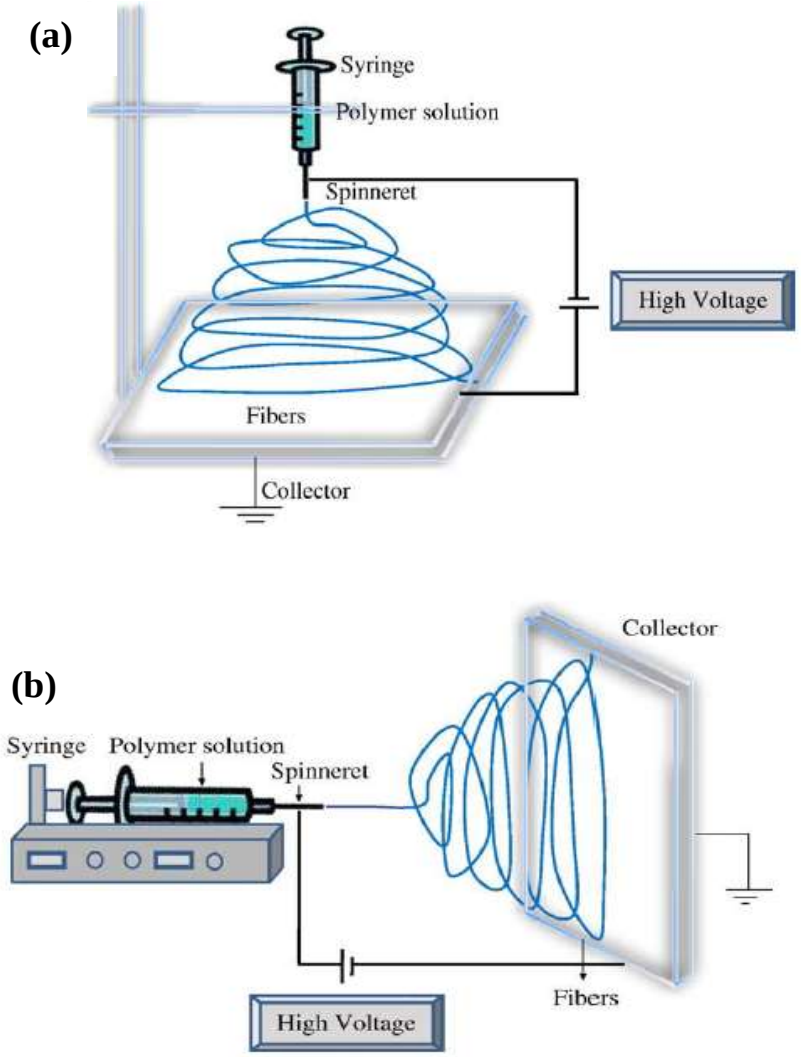

Figure 5: (a) Vertical setup and (b) Horizontal setup of the electrospinning process ; Source: (Bhardwaj and Kundu 2010)

There are three main components in the electrospinning setup: high voltage supply capable of generating a DC voltage in the range of a few tens of kV, spinneret or the needle from which the polymer enters the electric field, and a collector plate which is to collect the fibers during the process. All of these are also seen in the above figures of the vertical and horizontal setup. Once a polymer solution is prepared, it is loaded into the syringe and fixed to a flowmeter which controls the flow of the solution in the syringe. One end of the high voltage is

connected to the needle of the syringe and the other end is connected to the collector which is grounded. Thus we have a set-up which looks like the Figures 5(a) and 5(b) above. To start the electrospinning process, we turn on the flowmeter and then the voltmeter, thus producing an electric field in between the spinneret and the collector. Once the polymer solution pops out of the spinneret/needle, it is now held by its surface tension at the tip of the needle, subject to an electric field. This electric field induces an electric charge on the surface of the polymer and by increasing the intensity of the electric field, the repulsive electric forces overcome the surface tension forces and the semi-spherical surface of the polymer at the tip of the needle, elongates into a conical shape, which is the Taylor cone (Huang, Zhang et al. 2003). At a critical value of the electric field, a charged jet of solution is ejected from the tip of the Taylor cone causing an unstable whipping action of the jet in the space between the collector plate and the spinneret (Yarin, Koombhongse et al. 2001). During this travel of the jet in the space between the collector plate and the spinneret, the solvent in the jet evaporates, leaving behind the polymer fibers which randomly lay on the collector forming continuous fibers (Taylor 1969, Yarin, Koombhongse et al. 2001, Adomaviciute and Milasius 2007).

1.8.1 Parameters that effect electrospinning

There are various parameters that affect the electrospinning process and they can be broadly classified into two main groups: Solution parameters and Process parameters. By varying each of these parameters, we can achieve fibers of desired diameter and morphology (Chong, Phan et al. 2007), that are important factors which affect the efficiency of catalysts. The two groups of parameters are explained below:

1) *Solution Parameters*:

1a) Concentration

The concentration of a solution alters the diameter and morphology of fibers in such a manner that with a low concentration a mixture of beads and fibers are formed and with an

increase in concentration the spherical beads get elongated and spindle like fibers being uniform with larger diameters are obtained which are due to higher viscosity resistance (Deitzel, Kleinmeyer et al. 2001, Ryu, Kim et al. 2003, McKee, Wilkes et al. 2004). Since at lower concentration beads are formed and at higher concentrations (due to instability of the flow of the solution from the tip of the needle), larger fibers are formed there should be an optimum concentration at which continuous fibers are obtained (Sukigara, Gandhi et al. 2003). Ki et al. and Jun et al., have shown that there is a power law relation between concentration and fiber diameter for gelatin electrospinning, in which an increase in concentration of the solution increases fiber diameter (Jun, Hou et al. 2003, Ki, Baek et al. 2005). It is shown that surface tension and viscosity of the solution also play a vital role in deciding the range of concentrations for obtaining continuous fibers in the electrospinning process (Deitzel, Kleinmeyer et al. 2001).

1b) Viscosity

Viscosity plays an important role in electrospinning as it contributes to a large extent in determining the fiber diameter and morphology. At very low viscosity there is no continuous formation of fibers and with high viscosity there are problems in the ejection of jets during spinning, thus this calls to find out an optimum value for viscosity. There have been reports on the maximum range of viscosity for electrospinning to be from 1 to 215 poise (Baumgarten 1971, Doshi and Reneker 1995, Buchko, Chen et al. 1999, Deitzel, Kosik et al. 2002). However, there is a polymer specific optimum viscosity value for electrospinning. For example, it has been reported that PEO (polyethylene oxide) has an optimum viscosity range of 1 to 20 poise between which uniform nanofibers can be obtained (Fong, Chun et al. 1999). Viscosity, molecular weight and polymer concentration are parameters correlated to each other and their relationships with each have been studied using various polymers like PVA (Ding, Kim et al. 2002, Zhang, Yuan et al. 2005) , PEO (Son, Youk et al. 2004) and PLGA (Kim, Jeong et al. 2005). At very high viscosities, the polymer solutions have long stress relaxation times which tend to prevent the fracture of an ejected jet from the tip of the needle during electrospinning. When the viscosity of a polymer solution is low, there are problems of beaded fibers being formed, and when the solution concentration reaches a critical point, continuous fibers are obtained whose morphology is dependent on the concentration of the solution (Doshi and Reneker 1995).

1c) Molecular Weight:

Researchers have found out that the effects of molecular weight of a solution are extended to the rheological and electrical properties besides having an effect on the morphology and size of the fibers (Haghi and Akbari 2007). It has been noticed that solutions with low molecular weight, have difficulties in forming fibers and have a tendency to form beads. Solutions that are high in molecular weight are generally preferred for electrospinning, but again problems of large diameter of fibers are encountered. Studies have shown the effect of molecular weight on morphology of fibers where it is seen that as the molecular weight is increased the bead formation is decreased (Gupta, Elkins et al. 2005). It has been studied that polymers with high molecular weights are not absolutely necessary if intermolecular interactions can be a substituent to interchain connectivity obtained through chain entanglements. Based on this study non-woven membranes have been produced by electrospinning oligomer-sized phospholipids from lecithin solutions (McKee, Wilkes et al. 2004, Burger, Hsiao et al. 2006).

1d) Surface Tension:

It has been shown that surface tension of a solution can determine the upper and lower boundaries for electrospinning, keeping all other parameters constant (Fong and Reneker 1999, Zhang, Yuan et al. 2005). Surface tension depends on the solvents being used as different solvents cause different surface tensions. In general, solutions with low surface tensions eliminate the problem of bead formation and solutions with high surface tensions cause difficulties in electrospinning as there exists instability in formation of jets and formation of sprayed droplets (Hohman, Shin et al. 2001). Lower surface tensions are preferred as it also helps electrospinning with lower electric fields (Haghi and Akbari 2007).

1e) Conductivity:

The conductivity of a solution mainly depends on the type of polymer used, the solvent and the availability of ionisable salts. Most polymers are conductive having charged ions that are influential towards the formation of jets. It has been observed that with low solution conductivities, there is not enough electrical force to pull and elongate the jet to form uniform fibers and this may produce beads. With an increase in the electrical conductivity of the solution, fibers with significantly lower diameters can be formed. It has been studied that the radius of the

jet varies inversely to the cube root of the electrical conductivity of the solution (Huang, Nagapudi et al. 2001, Zong, Kim et al. 2002, Jiang, Fang et al. 2004, Mit-uppatham, Nithitanakul et al. 2004). Researchers have studied and demonstrated the effect of adding ionic salts (NaCl, NaH_2PO_4 and KH_2PO_4) on the conductivity of solutions. It was shown that by adding these salts, the conductivity of solutions increased leading to uniform formation of fibers with much smaller diameters and elimination of bead formation(Zong, Kim et al. 2002).

2) Process Parameters:

2a) Voltage

The voltage applied to the solution for electrospinning, is an important parameter since this initiates the electrospinning by forming a jet. Jet formation to form fibers, occur only after a certain threshold voltage is reached and this applied voltage also induces necessary charges on the solution besides the electric field, that all contribute to the initiation of the electrospinning process. There have been some conflicts over the years on the theory of the effects of voltage on the morphology or size of fibers. When researchers like Zhang et al., and Demir et al., have shown that higher voltages lead to larger fiber diameters because of more polymer ejection, others have argued that with higher voltages there would be smaller fiber diameters because an increased voltage, increases the electric field and that in turn increases the electrostatic repulsive forces on the jet which leads to thinner fibers (Demir, Yilgor et al. 2002, Zhang, Yuan et al. 2005). However in most solutions it is observed that with higher voltages there are stronger columbic forces in the jet which contribute to the high stretching of jets and also causes evaporation of solvent from the fibers, thus forming fibers of reduced diameters. Larrondo and Manley have shown that by doubling the applied voltage, the fiber diameter has reduces by almost half its size (Larrondo and Manley 1981). Thus we can conclude from all the research that voltage plays a significant role in electrospinning as it affects the fiber diameter, but it also varies with the solution concentration and the working distance (Yordem, Papila et al. 2008).

2b) Flow rate:

The flow rate or feed rate which is normally controlled by a flowmeter and is another significant parameter in the electrospinning process as it determines the velocity or rate of solution ejection from the needle. It has been reported that lower flow rates are desirable since it then provides enough time for solvent evaporation (Yuan, Zhang et al. 2004). Experiments on Polystyrene solutions have shown that with increase in flow rate, the fiber and pore diameter also increases and also showing a slight change in morphology. Many reports show how the fiber diameter and morphology are affected by varying the flow rate of a solution (Megelski, Stephens et al. 2002, Zong, Kim et al. 2002). Studies show that high flow rates lead to bead formation which is because of insufficient drying time from the tip of the needle and the collector (Wannatong, Sirivat et al. 2004, Kim, Jeong et al. 2005).

2c) Working Distance:

The distance between the tip of the needle and the collector is the working distance and this does have an effect on electrospun fibers. Like most parameters, there is an optimum distance that should be used in order to provide sufficient time for drying of the solvent from the tip of the needle to the collector to form good fibers. It has been observed that with either too small or too large working distances, both lead to beaded fibers (Lee, Choi et al. 2004, Geng, Kwon et al. 2005, Ki, Baek et al. 2005). Electrospinning with silk like polymers have shown to have formed flat fibers when the working distance was kept small and when the distance was increased round fibers were noticed (Buchko, Chen et al. 1999). Whereas for polysulfone, smaller working distance has worked the best (Pham, Sharma et al. 2006). Since dryness of a solvent used to form a solution for electrospinning is an important parameter, the distance between the tip of the needle and the collector should be kept at an optimum, to allow enough time for the evaporation of solvent to form nanofibers (Jalili, Hosseini et al. 2005).

3) Ambient parameters

Apart from the two main categories that is solution parameters and the processing parameters, ambient parameters like humidity and temperature also affect the electrospinning

process and must be taken into account. Experiments were conducted to check the effect of temperature of a polymer solution on the size and morphology of fibers formed from a polyamide-6 solution. It was seen that as the temperature of the solution increased, the diameter of the electrospun fibers decreased and this reduction in size was attributed to the viscosity of the solution which decreased due to the increase in temperature (Mit-uppatham, Nithitanakul et al. 2004). Humidity variations and their effects on electrospun fibers have been reported and it was shown that with high humidity levels, the fibers were seen to have small pores on their surfaces and with further increase in humidity, these pores were seen to coalesce (Casper, Stephens et al. 2004). At conditions of very low humidity, it was observed that there was rapid evaporation of the solvent, as a volatile solvent dries faster in this condition. Thus, it is important to control the humidity and temperature of a solution besides the solution and processing parameters, as these also contribute to the size and morphology of fibers.

1.9 Methylene blue

Methylene blue dye was discovered by Caro in 1878 (El Qada, Allen et al. 2006) and has been most commonly used as a model dye for adsorption of organic dyes from aqueous solution (Chandrasekhar and Pramada 2006). It is a heterocyclic aromatic chemical compound have a molecular formula : $C_{16}H_{18}N_3SCl$ (Jian-xiao, Ying et al. 2011). The structure of methylene blue is as shown below:

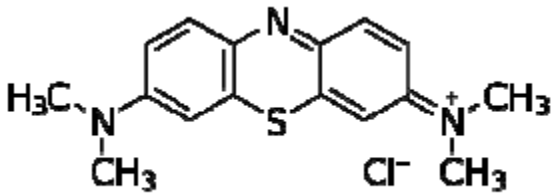

Figure 6: Crystal structure of methylene blue
Source: (Jian-xiao, Ying et al. 2011)

Methylene blue dye is widely employed in industries such as food industries, textile industries, chemical industries and also being used in the medical field (Gillman 2006, Gillman 2008). As in the textile industry, MB is used for dying cottons, coloring of paper, hair colorants, dying wool, silk, and so on. In the chemical field it is used as peroxide generator, an oxidation-reduction indicator to cyanide, a stain in bacteriology and as a veterinarian antiseptic. It has also been used widely to treat diseases such as cancer(Schirmer, Coulibaly et al. 2003), psoriasis(Salah, Samy et al. 2009), malaria(Meissner, Mandi et al. 2006), etc.

Despite its various applications, methylene blue is considered as harmful since it causes certain problems like vomiting, increased heart rate, shock, tissue necrosis, quadriplegia, cyanosis and jaundice (Zendehdel, Barati et al. 2010). It poses a threat to the environment, as it is a common dye which is found in effluents that contaminant water. Therefore, it becomes important to remove it from the wastewaters, thereby degrading it into inorganic compounds. One is the methods to achieve this is by adding a photocatalyst (Houas, Lachheb et al. 2001, Tang, Zou et al. 2003, Kwon, Shin et al. 2004, Lin, Huang et al. 2006) which breaks up the MB structure, thus degrading it into harmless products. Titania, a commonly used photocatalyst, completely mineralizes MB by using oxygen from air. TiO_2 also photo-oxidizes acid blue dye which is used in textile industries according to:

$C_{16}H_{18}N_3SCl + 25.5O_2 \rightarrow 16CO_2 + 6H_2O + 3HNO_3 + H_2SO_4$

Source:(Salem and El-Maazawi 2000)

1.10 Industrial standards to measure methylene blue degradation

The ISO industrial standards to measure the photocatalytic degradation of methylene blue solution uses a sample plate($10cm^2$, with active coating) preconditioned by exposing it to UVA light for a certain amount of time, onto which a glass cylinder (3-4.7cm diameter) is fixed. Into this system a conditioning solution of 35ml methylene blue solution $2x10^{-5}$ M MB^+ is poured and left in the dark for 12 hours. In case the $[MB^+]$ is lesser than 10^{-5}M after 12 hours, then the step is repeated using a fresh MB solution. If this is not the case, then the 35ml solution is covered with a UV transparent glass side and irradiated with UVA light (1.0 mW/cm^2) agitating the

solution every 20 minutes. The solution was irradiated for 3 hours, at a reaction temperature of 23 ± 20C. A blank solution (in dark) was also run simultaneously (Mills, Hill et al. 2012).

The entire industrial set up was not followed in this research since we encountered delays in receiving the UV glass slides and glass cylinders. Also when several experiments had to be conducted, keeping the solution for 12 hours in the dark was time consuming, so previous literature research work was followed.

CHAPTER 2: MATERIALS USED

In this thesis, pure titanium dioxide, copper doped titanium dioxide and copper doped degussa P25 titanium dioxide were synthesized. The chemicals used for preparation are listed below in the Table 2.

Table 2: Properties of chemicals used in the synthesis of photocatalyst

Chemical Name	Chemical Formula	Molar Mass (g/mol)	Company	Density (g/cm^3)
Titanium(IV) Isopropoxide	$Ti[OCH(CH_3)_2]_4$	284.22 (97% purity)	Alfa Aesar	0.937
Polyvinylpyrrolidone	$(C_6H_9NO)n$	2.5	Sigma-aldrich	1.2
Titanium(IV) Oxide	TiO_2	79.86	Sigma-aldrich	4.23
Copper(II) Nitrate Trihydrate	$Cu(NO_3)_2.3H_2O$	241.60	Sigma-aldrich	3.05
Ethyl Alcohol	CH_3CH_2OH	46.06	Pharmo-Aaper	0.789
Acetone	CH_3COCH_3	58.08	Pharmo-Aaper	0.791
Acetic Acid	CH_3COOH	60.05	Pharmo-Aaper	1.05

CHAPTER 3: METHODS OF PREPARATION

The photocatalysts prepared and tested in this thesis, could be broadly grouped into three sections:

1) Synthesis of :
    a) Pure titania fibers
    b) Copper doped titania fibers
    c) Copper doped degussa P25 TiO_2

2) Characterization

3) Photocatalytic activity tests

For the preparation of the three synthesized photocatalysts in this thesis, three general steps were followed: the first was to prepare the sol-gel solution for electrospinning, second was to electrospin the solution to form fibers and third was the heat treatment of collected fibers.

3.1 Preparation of pure titania photocatalyst

First a 7.5ml of PVP solution containing 5% PVP was prepared. This was done so by adding 0.45g of PVP in 7.12ml Ethanol and this mixture was ultrasonicated for about an hour or till it dissolved and became a one phase solution. Then, in a glove box filled with Nitrogen, 1.6ml of Titanium Isopropoxide (TIP) was added to a mixture of 3ml Acetone and 3ml Ethanol. This mixture was left undisturbed for about 15 minutes in the glove box. This solution was then removed from the box and poured into the 7.5ml polymer solution and this final mixture was ultrasonicated for about 1 hour till a transparent homogeneous light yellow solution was achieved. This prepared yellow solution was called the spinning solution.

Though there are several other polymers used, PVP was chosen since it easily dissolves in water and in alcohol and most importantly even though it has a very high average molecular weight of 1300000, it is compatible with Titanium Isopropoxide, a Titania precursor. Acetic Acid was added along with the solvent Ethanol, so it would stabilize the solution when TIP was added and get the hydrolysis of the sol-gel precursor under control.

Once the spinning solution was ready, it was immediately transferred into a 10ml plastic syringe having a blunt 22 gauge stainless steel needle. This syringe with the solution was fixed to a Kd Scientific flowmeter that was functioned to operate at a flowrate of 0.030ml/minute. A collector which was a $20cm^2$ glass plate covered with aluminum foil, sprayed with Teflon (to help smoothly peel off the collected fibers from the foil after electrospinning), was kept at a distance of 10cm from the tip of the needle. In order to apply an electric field which is required for the electrospinning process, a Gamma High Voltage Research DC Voltmeter capable of producing voltages up to 30kV was used. The emitting electrode of the voltmeter was connected to the needle and the grounding electrode was connected to the collector plate. Once all this was set-up, the flowmeter was started and immediately the voltmeter was turned on in order to start the electrospinning process to produce nanofibers. According to the humidity conditions at the time of the experiment, the voltage that was to be applied between the needle and the collector was varied between 12kV and 15kV.

The electrospinning process went on for about 6 hours and during the process, the set up was constantly monitored to check if the solution was spinning rightly or if it stopped electrospinning due to a clogged needle. In that case, the voltage was turned off and the needle was cleaned and fixed back into the syringe to resume the electrospinning process.

Once the entire solution in the syringe was electrospun, the fibers were peeled off from the collector plate and placed in a tube furnace for heat treatment. Since the fibers cannot be directly put into the glass tube of the furnace, it was put in aluminum foil which was rolled in the shape of a tube so when this rolled foil with the as-spun fibers was kept in the tube furnace, there would be enough room for air to travel through the rolled foil and thus being available for the annealing of the fibers. The furnace was functioned so that it operated to raise its temperature from 25^0C (room temperature) to 450^0C in 90 minutes, stayed at 450^0C for 30 minutes that was

its dwell temperature and then dropped to 25^0C in 90 minutes. The annealed fibers –the photocatalysts, were taken out from the furnace and ready to be tested for their efficiencies.

3.2 Preparation of copper doped titania photocatalyst

In the case of doping titania with copper, 5 atom weight percent of copper with respect to titanium, was decided to be used for doping after a literature review of the doping levels and their effects. So, the procedure was to make a 4ml, 10% PVP solution by adding 0.48g of PVP in 3.6ml Ethanol. Ultrasonicate this solution for an hour till all the PVP dissolves and a one phase solution is seen. In a separate vial, add 0.084g of $CuNO_3$ to 2ml Acetic Acid and ultrasonicate it for 10-15 minutes till all the $CuNO_3$ crystals dissolve. In a nitrogen glove box, add 2ml of Titanium Isopropoxide to this above solution of $CuNO_3$-Acetic Acid. Leave this undisturbed for about 15 minutes. Take it out of the glove box and then ultrasonicate this TIP-$CuNO_3$-Acid mixture for 30 minutes. Then pour this above homogeneous solution into the initially prepared PVP solution and ultrasonicate this for one and half hours till a homogeneous greenish-blue sol is seen. Immediately transfer this spinning solution into a syringe and start electrospinning.

All the details of the electrospinning process are the same as explained above for Preparation of Pure Titania. A 22 gauge needle was used and the process parameters were kept so that the flowrate was 0.045ml/minute, working distance of 15cm and voltage was between 17kV and 20kV.

The as spun fibers were heat treated in the same way as the pure titania fibers that is in the tube furnace at 450^0C for 30 minutes. The photocatalysts were then checked for their activity with methylene blue dye solution under UV and visible light.

3.3 Preparation of copper doped degussa P25 TiO_2 photocatalyst

It was chosen to dope degussa P 25 with 5 atom weight percent copper so we could have a comparison of this with the 5 atom weight percent copper doped titania from TIP. In order to make the preparations for this, a 7ml PVP solution was prepared by adding 0.48g of PVP in 6.6ml Ethanol. Ultrasonicate this solution for an hour till all the PVP dissolves and a one phase solution is seen. In a separate vial, add 0.152g of $CuNO_3$ to a solution of (2ml Acetic Acid and 3ml Acetone), ultrasonicate it for 10-15 minutes till all the $CuNO_3$ crystals dissolve. Then add 1g of degussa P 25 TiO_2 to this above $CuNO_3$ solution and ultrasonicate for 30 minutes till all the particles are dissolved. Now pour the initially prepared PVP solution into the above TiO_2 - $CuNO_3$ solution and ultrasonicate for one and half hours. Immediately transfer this spinning solution into a syringe and start electrospinning.

All the details of the electrospinning process are the same as explained for the Preparation of Pure Titania. The process parameters were kept so that the flowrate was 0.045ml/minute, working distance of 15cm and voltage was between 17kV and 20kV, using a 20 gauge needle, since the spinning solution was more viscous.

The as spun fibers were heat treated in the same way as the pure titania fibers that is in the tube furnace at 450^0C for 30 minutes. The photocatalysts were then checked for their activity with methylene blue dye solution under UV and visible light.

Thus, three photocatalysts were synthesized by the materials and methods discussed above and then characterized using the SEM, TEM and XRD instruments. Finally they were tested for their photocatalytic activity with methylene blue solution under UV light and visible light, along with the degussa P25 photocatalyst, to check which of the synthesized photocatalysts would work better that the commercially available degussa.

CHAPTER 4: CHARACTERIZATION TECHNIQUES

4.1 SEM

It is important to analyze, observe and understand materials at a microscopic level. The scanning electron microscope is one of the many instruments that serve this purpose. The beam of electrons is scanned in a raster scan pattern and the electron beam's location is combined with the detected signal, to produce an image. The electrons of the beam interact with the atoms of the sample material, producing signals containing information of the sample's topography, composition and properties like electrical conductivity and more. With the Scanning electron microscope, resolutions higher that 1 nanometer can be achieved. Due to its narrow electron beam, images with high depth of field can be taken, which are very helpful in understanding the structure of the material.

The type of signal used for detection of all the images taken in this work was the back scattered electrons (BSE). These are electrons reflected from the sample by elastic scattering. BSE are related strongly to the atomic numbers of elements. BSE are the best signals to be used in order to obtain information on the distribution of various elements of the sample. When an electron beam strikes an atom of the sample (removing an inner shell electron and refilling this by a higher energy electron), it produces a characteristic X- ray. These X-rays are used to detect the elements of the samples and the abundance of it, thus giving us an EDAX (Energy Dispersive X-Ray Analysis) image.

All the samples were coated with a thin layer of gold, an electrically conductive material, since it increases the signal to noise ratio for samples of low atomic number, thus producing images with good contrast. A very tiny quantity of sample is required for the SEM analysis. The gold coated samples were mounted rigidly on a sample holder by the help of thin carbon tapes to hold the samples in position.

A LEO 1550 Schottkey Field Emission Scanning Electron Microscope was used to analyze the nanomaterial photocatalysts. The analysis was done in order to get information on the size of the nanofibers and morphology of the materials. A working distance of 8mm, EHT of 20 kV and back scattered signal was used for all the images.

4.2 EDS

The Energy Dispersive X-Ray Spectroscopy is a quantitative analysis technique that measures line intensities of X-rays produced upon the electron irradiation of the material and which are characteristic of its composition (i.e. provides elemental analysis). X-rays that are emitted by a sample upon bombardment by a beam of electrons are made use of to obtain localized chemical information. Almost all the elements listed in the periodic table can be identified by this principle. This is used to determine the concentration of the elements present in the sample by identifying lines in the spectrum. This is a straight forward methodology since it deals with X ray spectra.

Images or maps of the distribution of elements are produced when a beam is scanned in a television like raster, displaying the intensities of the selected x-ray lines. It can be thought of as a pixel by pixel imaging based on the chemical elements of the sample. The collected electrons that form the image carry information about the surface topology or mean atomic number differences depending on the mode selected.

4.3 TEM

The Transmission Electron Microscopy is a characterization method in which a beam of electrons pass through a sample. While it passes through, the beam interacts with the components of the sample and the electrons transmitted through the sample form the image. The image is then magnified and focused onto an imaging screen. TEM images are formed with very high

resolutions and provide information on the internal composition of the sample. It provides characteristic details such as particle shape, crystallization, stress, morphology and even magnetic domains. TEM imaging is used for identifying dislocations, grain boundaries, very small precipitates and other structural defects in solids. TEM is used as a powerful imaging method when atom distributions in nanocrystals coated or containing polymers are to be imaged.

The TEM used in this work was JEOL 1400, and a copper grid was used for the sample preparation. The BF mode was used to study the images.

4.4 XRD

X-Ray Diffraction is an analytical technique that helps to examine the phase of a crystalline material and also provides information on the dimensions of unit cells. Since 95% of the materials are crystalline, XRD becomes a very useful and common chemical analysis for characterization of samples.

When an X-ray hits the specimen or the crystalline phase, it interacts with it and produces a diffraction pattern. Every crystalline phase produces a diffraction pattern and the same substance produces the same diffraction pattern every single time. For a mixture of phases in a sample, each phase produces its pattern independently of each other (Hull 1919). Thus, the diffraction patterns are like finger prints for each phase.

For the sample preparation, the samples are powdered finely and put into a sample holder which is then fitted into the X-ray Diffractometer. The machine is then turned on using the generator button and the current and voltage are increased slowly to reach a value of 30mA and 40kV respectively. The X-plot software is set up so that it records patterns starting from 20^0 to 80^0 in steps of 1^0 per minute. When a scan starts, the shutter is opened allowing X-rays of a fixed wavelength to interact with the sample producing diffraction patterns and the intensity of the reflected radiation is recorded using a goniometer. The areas under the peaks reflect the amount of that phase present in the sample.

There have been 25000 organic and 50000 inorganic single component crystal phases with their distinct diffraction patterns that have been collected over the years and stored as standards. The prime purpose of diffraction is to help identify unknown components in a sample by a search and match procedure using XRD cards that contain information of materials.

A Philips X-Ray Diffractometer was used to characterize the photocatalysts and the software XPlot version 1.38 was used for plotting data along with PC-1710 version 2.0 for acquisition.

Photocatalytic test

Photocatalytic experiments were carried out for pure titania nanofibers, copper doped titania nanofibers, degussa P25 TiO_2 nanoparticles and copper doped degussa TiO_2 nanoparticles. Each of these were studied for their photocatalytic efficiencies under UV light and under visible light separately. A solution of methylene blue was analyzed for its degradation by activity of these catalysts on illumination of light.

In a typical experiment, 0.018g of the catalyst was added to a 4ml methylene blue dye solution of 50ppm concentration (0.2mg of methylene blue dye in 20 ml water). This was kept in the dark for 1 hour to obtain an adsorption-desorption equilibrium. Before the solution was kept under the UV or visible light, about 2ml of the sample was pipetted out to make an absorbance measurement which was recorded as 0 minutes absorbance. A Newport Ultraviolet light source with a 60W light bulb was used as the source for UV light and visible light (by using a 400nm filter in the same set up). The solution was then kept under the UV or visible light for 3 hours. Every hour 2ml of the solution was taken out to measure its absorbance value with the spectrophotometer. Care was taken to only pipette out the solution and not the catalyst particles while taking measurements. The degradation of methylene blue was evaluated by studying the changes in the absorbance value at a wavelength of 665nm, for every measurement made in the spectrasuite software.

4.5 UV-Vis spectroscopy

Ultraviolet-visible absorption spectroscopy is used to determine or measure the weakening in a beam of light after it passes through a sample. The light used for this purpose emits light intensities consistent in the UV region that is 190nm to 380nm and also in the visible range of 380nm to 800nm. When light passes through a sample the absorbance of it is directly related to the perceived color of the chemicals involved in that sample. In that area of the spectrum, molecules undergo electronic transitions. When sample molecules have energies that match the energy of light passed through it a certain amount gets absorbed due to electron jump to a higher energy level. The wavelength of absorption and the intensity of absorption at each wavelength are recorded by an optical spectrometer. The result is a plot of absorbance (A) against wavelength.

UV-Vis spectroscopy works on the principle that a molecule having π electrons or the n-electrons (non-bonding electrons), can absorb energies that are in the ultraviolet and visible range and become excited promoting these electrons to higher anti-bonding molecular orbitals. The easier an electron gets excited, longer will be the wavelength of absorbed light.

4.5.1 UV-Vis spectrometer

The instrument used for UV-Vis spectroscopy is the UV-Vis spectrophotometer. The function of this spectrophotometer is to record and compare the intensity of light that passes through a sample (I) and the intensity of light before passing through the sample (I_0). The ratio of I/I_0 is called transmittance (T), usually expressed as a percentage. The relationship between absorbance (A) and transmittance (T) is given by:

$$A = - \log (\%T/100\%)$$

The essential parts of a spectrophotometer are: a light source to generate UV or visible light, a diffraction grating or a prism to split the different wavelengths of light, a sample holder to hold the sample during measurement and a detector to sense the absorbed or reflected light. A typical set-up is shown in the figure below:

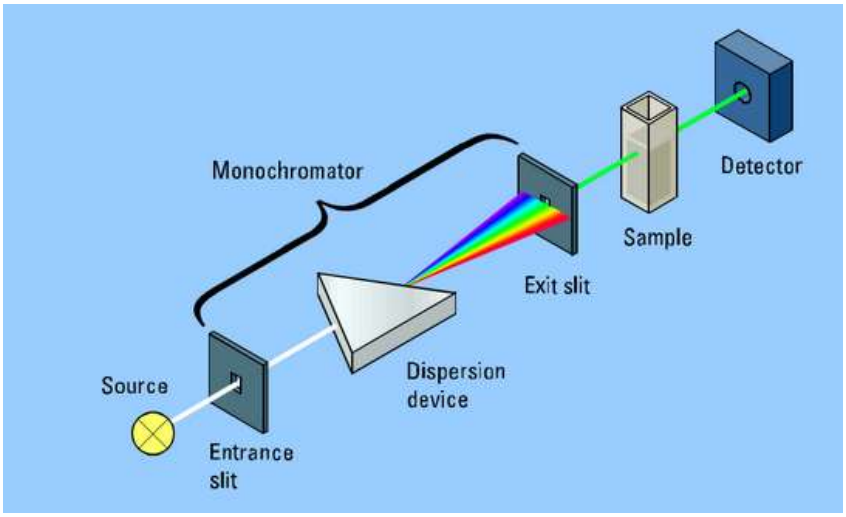

Figure 7: UV-Vis spectrophotometer (Source:(Owen 1996))

The spectrophotometer used in this project was Ocean Optics model HR 4000, which used a halogen and deuterium lamp for visible and ultraviolet light generation respectively and the software used to analyze the data was SpectraSuite. The absorbance mode was selected for all the sample measurements. Initial readings for an experiment required a light and dark reference spectrum to be recorded which was done using distilled water as the reference sample. After this reading was made, the actual sample was put in the sample holder and measured for its absorbance.

CHAPTER 5: RESULTS AND DISCUSSIONS

5.1 Color and flexibility of fibers

Pure titanium dioxide nanofibers and copper doped titanium dioxide fibers were synthesized using the electrospinning method as explained in the previous chapters. There is a difference in texture between the as-spun fibers (fibers from electrospinning without any processing, example: heat treatment) and the heat treated fibers. The heat treated fibers of pure titania and copper doped titania are shown in the Figure 8 below:

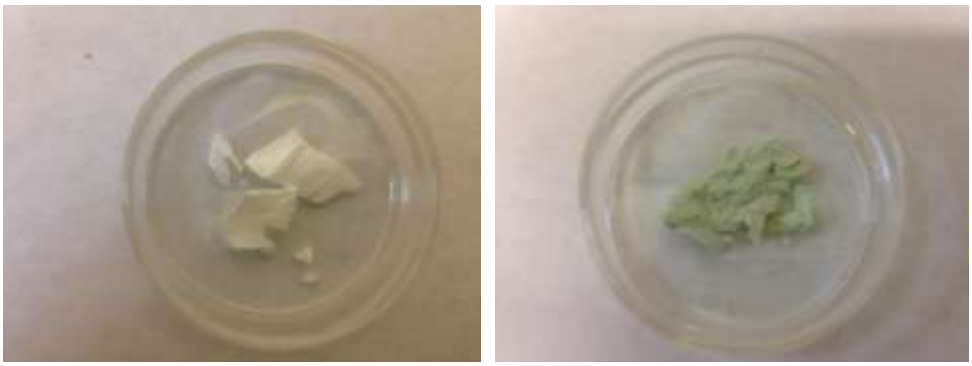

Figure 8:Heat treated fibers of pure titania and copper doped titania

The as-spun fibers of copper doped titania are whitish-blue in color (due to the blue color $CuNO_3$ spinning solution) and the heat treated ones are greenish-yellow in color. These differences in color before and after heat treatment of both the synthesized catalysts can be attributed to the loss in polymer content by heat treating the as-spun fibers to 450^0C. Also it was observed that the as-spun fibers are more flexible than the annealed fibers, and this can be attributed to the formation of crystalline phase on heat treatment of the fibers and loss in polymer content.

5.2 Characterization with the SEM and EDAX

To study and analyze the differences in the morphology of fibers before and after annealing, SEM images were taken. Figure 9(a) shows the SEM images of as-spun pure titania and Figure 9(b) shows pure titania after heat treatment. Both the images were taken under the same conditions of working distance, signal, EHT and a magnification of 100,000 times.

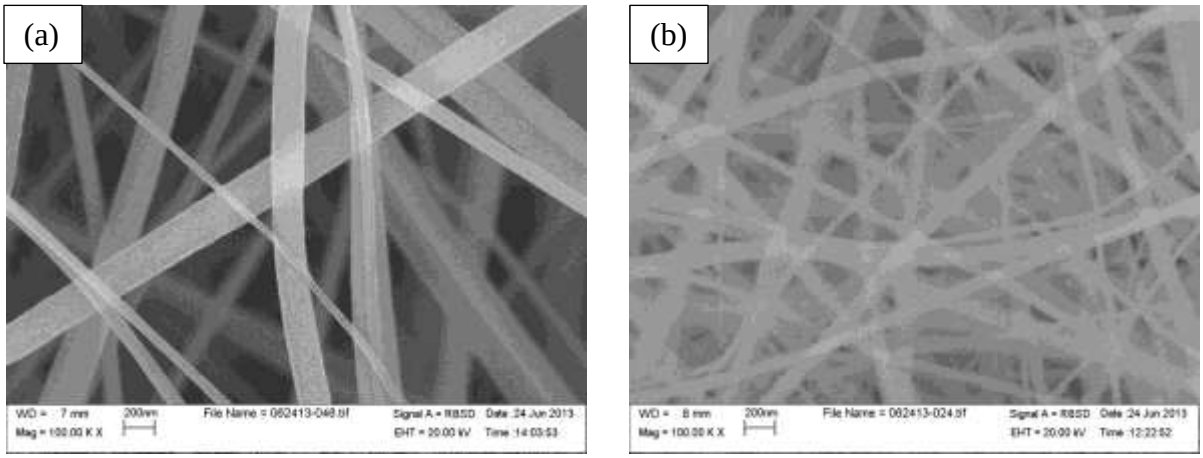

Figure 9: (a) As-spun fibers of pure titania; (b) Heat treated fibers of pure titania

The differences in morphology and size of fibers can be observed in both these images. The as-spun fibers have diameters in the range of 200-250nm which are larger than the heat treated fibers which have diameters in the range of 100-150nm. This decrease in size of the fibers after heat treatment is because of the loss of polymer during heating. The as-spun fibers contain a good amount of polymer in them since the spinning solution was prepared by a good amount of polymer solution. The polymer used in this work was PVP which has a melting point of 150^0C and as we heat treat the fibers to 450^0C, most of the PVP melts away during this annealing process and this points out to the decrease in size of the annealed fibers.

Another noted morphological difference is the smoothness of fibers in the as-spun fiber image. These seem to have well defined and smooth outline of fibers contrary to the annealed fibers that seem to have rougher outlines or edges. This difference in morphology can be attributed to the formation of crystal phase during heat treatment.

EDAX analysis was done on both the fibers to analyze the carbon content before annealing the fibers and after annealing. Since the amount of polymer is a direct measure of the carbon content, it was necessary to run EDAX on the fibers. The EDAX of as-spun fibers and heat treated fibers are shown in Figure 10 and Figure 11 below:

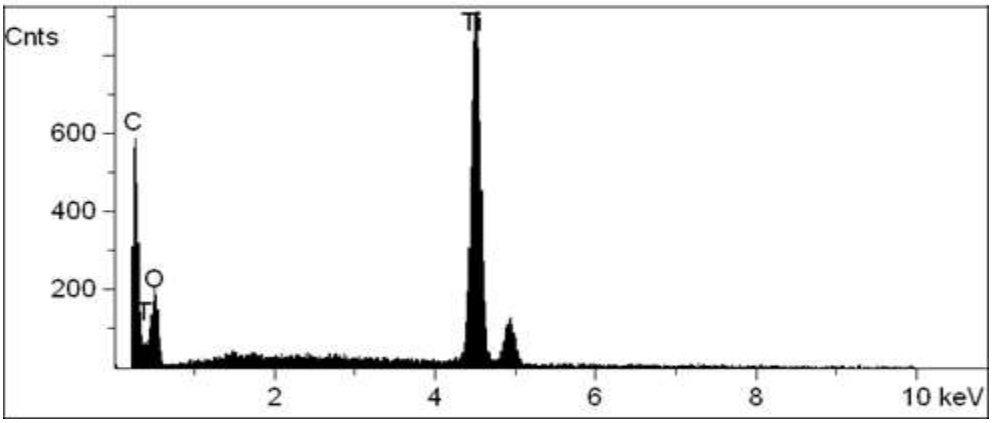

Figure 10: EDAX of as-spun pure titania fibers

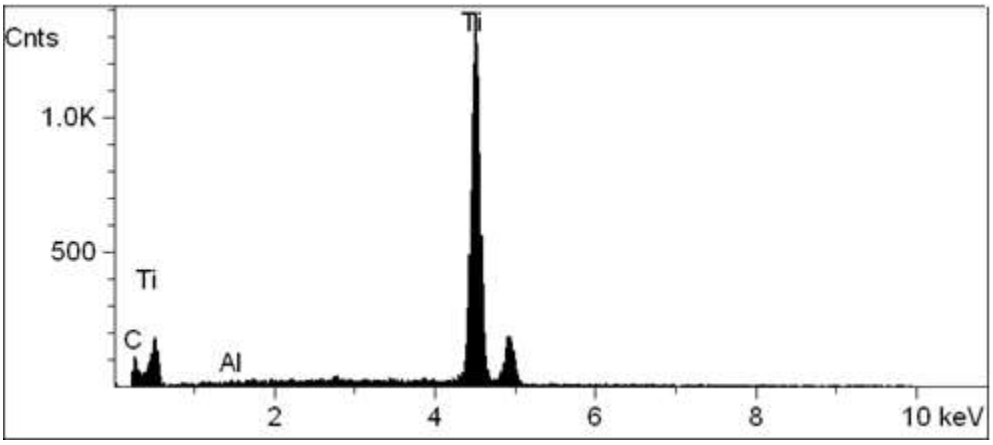

Figure 11: EDAX of heat treated pure titania fibers

It can be observed that the carbon peak is high in the as-spun EDAX image and much lower in the heat treated fibers EDAX image.

The SEM images of copper doped titania fibers before heat treatment and after heat treatment are shown in the Figure 12 (a) and (b) below.

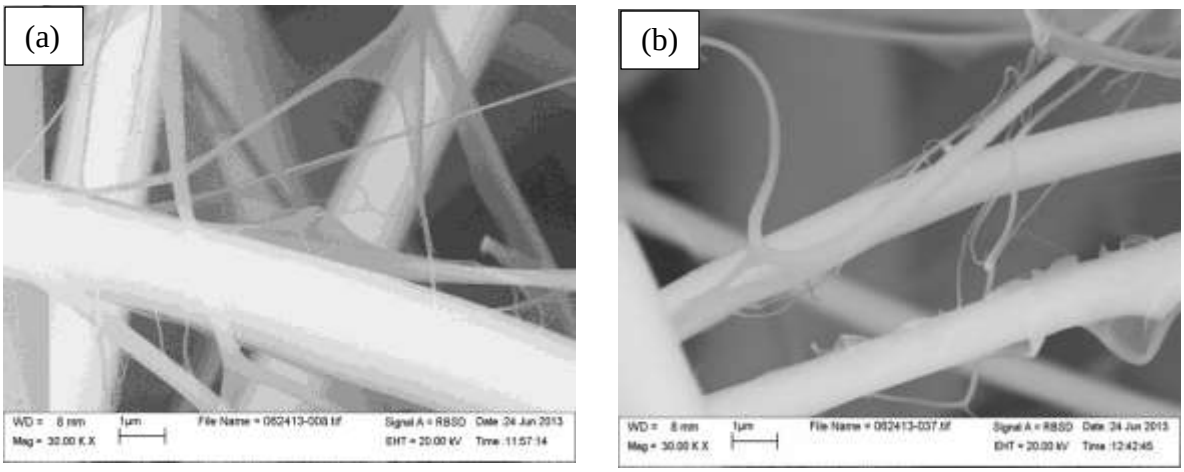

Figure 12: SEM images of (a) As-spun copper doped fibers; (b) Heat treated copper doped titania fibers

We can see that the as-spun fibers are slightly larger in diameter than the heat treated fibers. Also the thin translucent areas in both the images above are mostly the polymer fibers and it can be observed from the SEM images that there is more polymer in the fibers before heat treatment. Since a measure of carbon content is directly related to the polymer content, it was essential to carry out EDAX analysis so it would support the claim of polymer loss. The Figure 13 below show the EDAX of copper doped Titania fibers before annealing and Figure 14 shows the EDAX of it after annealing.

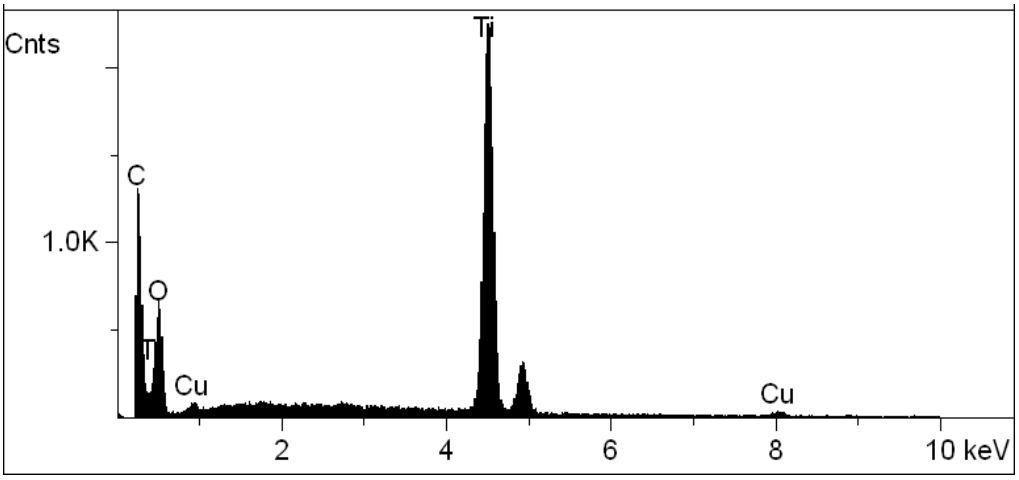

Figure 13: EDAX of as-spun copper doped titania fiber

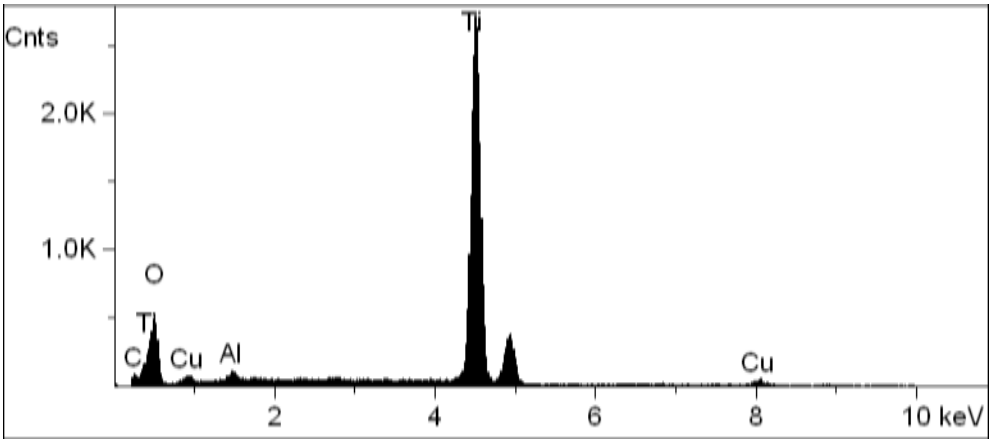

Figure 14: EDAX of heat treated copper doped titania fibers

It can be observed that the polymer content shown by the carbon peak in the Figure 13 is much higher than the carbon peak of the Figure 14, after heat treatment. Therefore the difference in carbon content analyzed in the EDAX images for as-spun fibers and heat treated fibers support our reason that there is a loss of polymer content due to decrease in fiber diameter.

SEM images of the three synthesized photocatalysts that is pure titania, copper doped titania and copper doped degussa P25, annealed at 450^0C for 30 minutes, each with a low and high magnification is shown in Figure 15, Figure 16 and Figure 17 below.

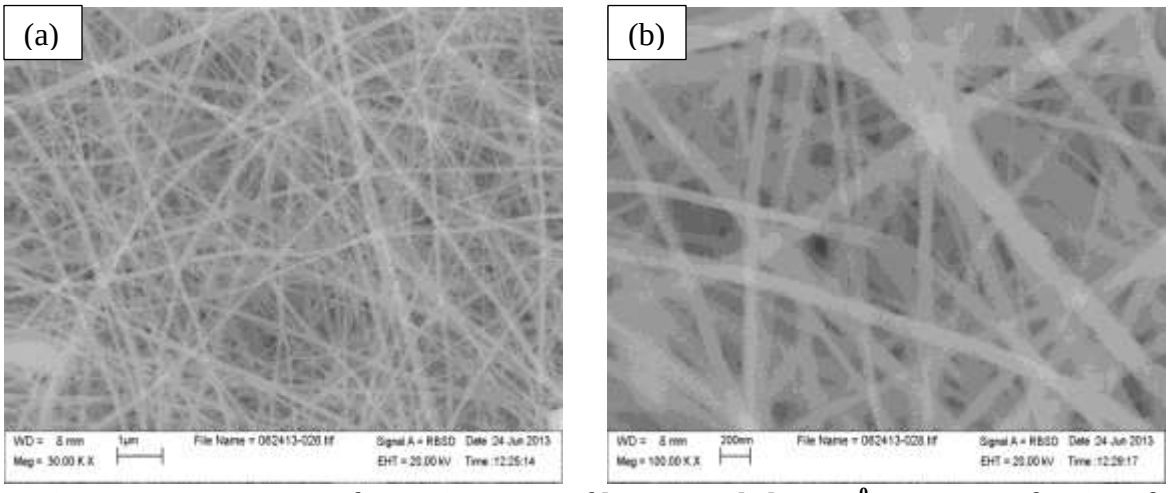

Figure 15: SEM images of pure titania nanofibers annealed at 450^{0}C at a magnification of (a)30K X and (b)100K X

The annealed pure titania nanofibers have small diameters in the range of 50-150nm. It is essential to have nano sized fibers since the efficiency of a photocatalyst is affected by the size of its fibers. Smaller the fiber or particle size, higher is the surface area and this is an important factor for a good catalyst and is has been achieved for pure titania catalyst.

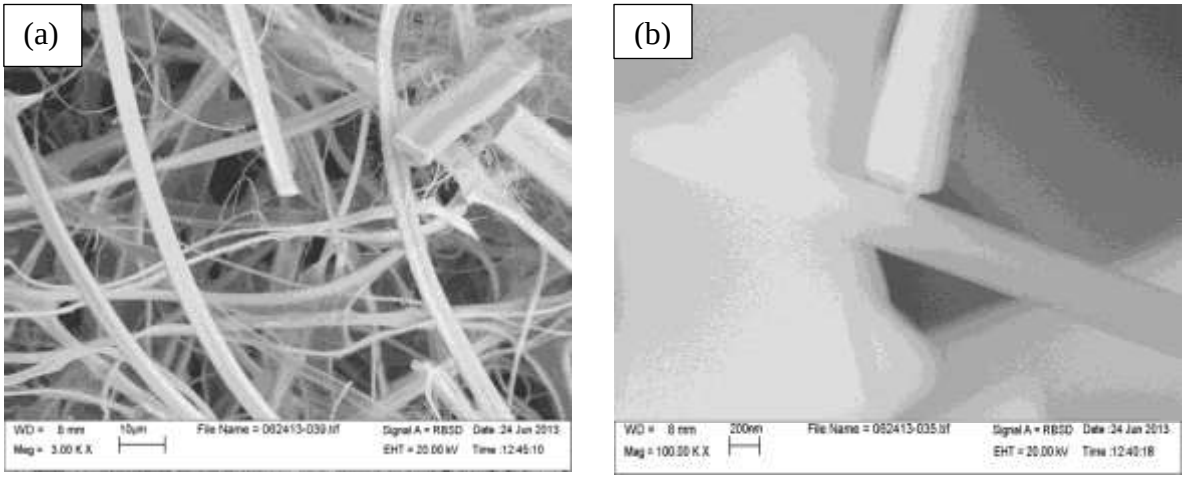

Figure 16: SEM images of copper doped titania annealed at 450^{0}C at a magnification of (a) 3 KX and (b) 100 KX

The Figure16(a) is the SEM image of the copper doped titania fibers which have a morphology that looks concave or as if two fibers are stuck together. This morphology of fibers is presumably caused due to the formation and collapse of jets during electrospinning (Arinstein and Zussman 2007). The volatility of a solvent plays an important role in the formation of fibers since by evaporation of the solvent and solidification of jets, fibers are formed. The only solvent used in the preparation of the spinning solution for this catalyst is acetic acid. Acetic acid has a high volatility rate causing the evaporation from the surface of the jet to occur rapidly forming fibers while the inside of the fibers are not. This could possibly lead to the formation of hollow fibers which collapse to form the concave morphology. The size of these fibers are in the range of 400-600nm much larger than the pure titania fibers. There were experimental difficulties while electrospinning this solution since the spinning sol was more viscous and the jet constantly solidified at the tip of the needle. This led to solidification of solution in the needle and hence blockage of the needle, which had to be cleaned to proceed with electrospinning. Therefore in order to overcome these difficulties we had to choose process parameters that allowed us to electrospin without much difficulty while still keeping in mind the need to reduce fiber diameters. This led to choosing process parameters that gave us fibers in range of 400-600nm, but still effective as a photocatalyst.

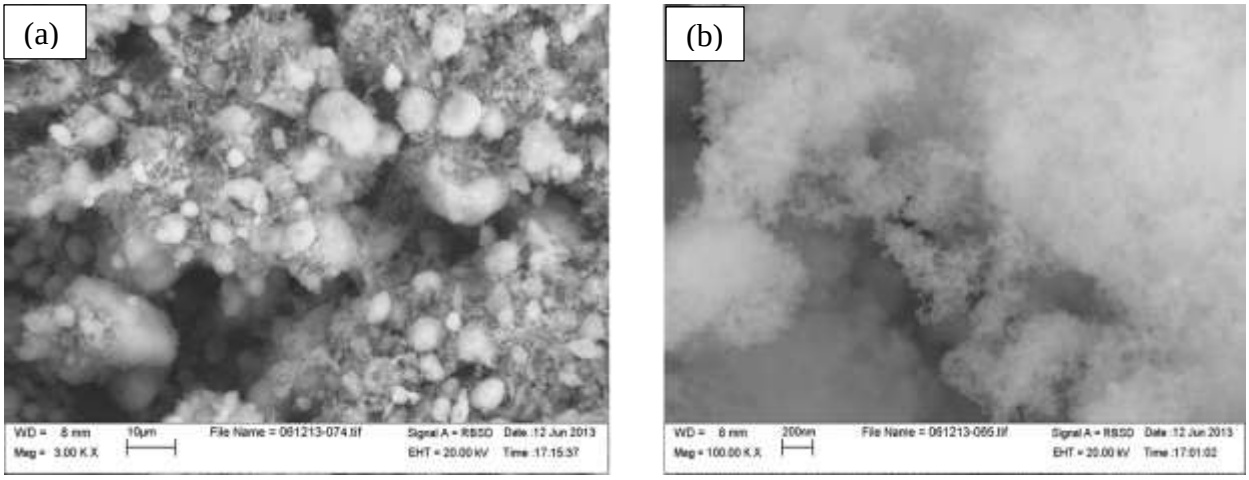

Figure 17: SEM images of copper doped degussa P25 annealed at 450^{0}C at a magnification of (a) 3 KX and (b) 100 KX

The above Figure 17 shows the SEM images of copper doped degussa TiO_2 photocatalyst. These are nanoparticles and not fibers, since in the preparation of spinning solution degussa TiO_2 powder was used. Electrospinning was the processing method chosen for even this catalyst since we were able to achieve a very fine smooth powder on heat treatment of the electrospun material. This fine powder was not obtained when the solution was directly heat treated without elctrospinning and the product obtained from this direct heat treatment were hard crystals around 3mm in size which gave an unsatisfactory response for photocatalytic activity tests. From the SEM image above of the copper doped degussa TiO_2, it can be inferred that they are very tiny particles in the nanometer range and thus have high surface area which could be a reason to enhance photocatalytic activity. The EDAX image of this photocatalyst is shown below:

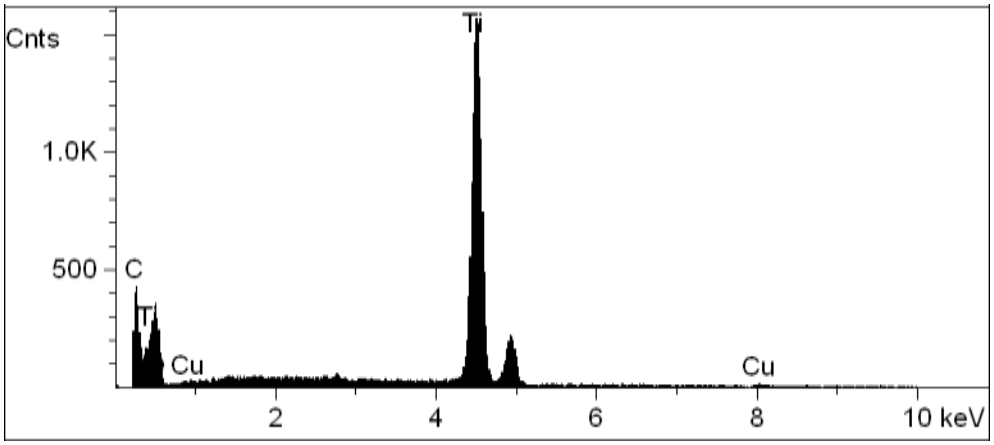

Figure 18: EDAX of copper doped degussa annealed at 450^0C

5.3 Characterization using TEM

The samples with nanofibers were characterized using the TEM. Figure 19 shows the TEM image of pure titania nanofibers at two different magnifications.

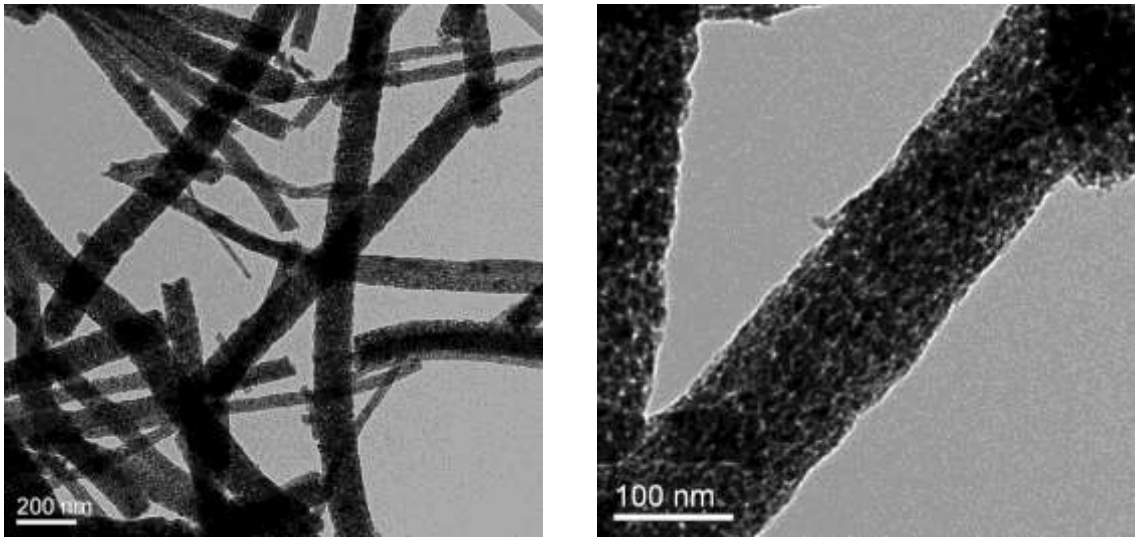

Figure 19: TEM images of pure titania nanofibers annealed at 450^{0}C at different magnifications

It is observed from the TEM images that this photocatalysts has a polycrystalline nature with fibers in the range of 100nm.

The TEM image of copper doped titania is show in Figure 20 below:

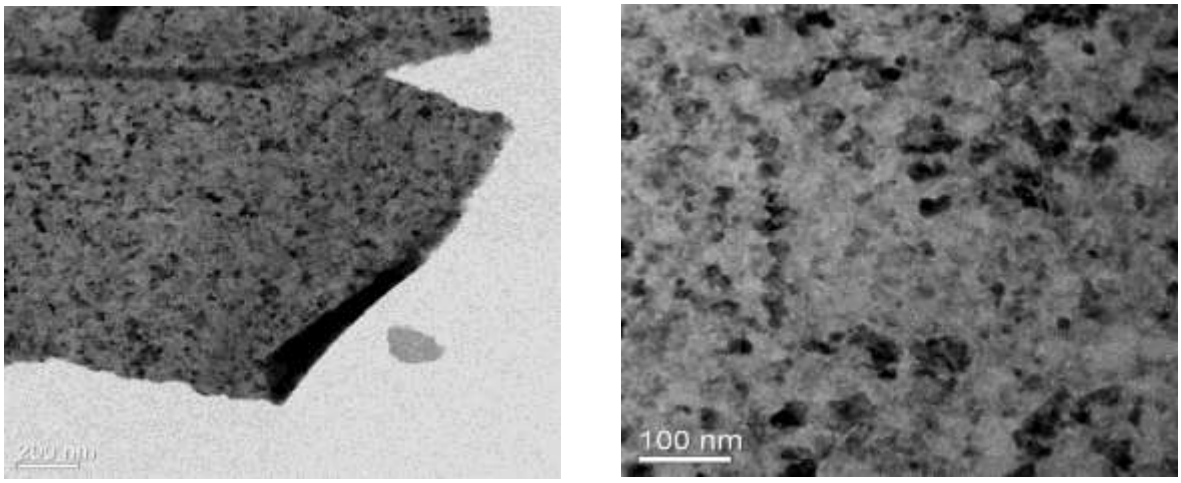

Figure 20: TEM images of copper doped titania fibers annealed at 450^{0}C

The TEM images above clearly show light and dark areas unlike the image for pure titania which had a uniform color for all its crystals. It can be inferred from the difference in colors that there are two different elements present. It appears as if darker particles are embedded in a sea of lighter particles. This provides evidence of the presence of a dopant used and in this case copper has been used as a dopant with Titania. Also the image represents a uniform distribution of copper particles. To confirm and verify the presence of copper particles, EDS mapping was performed.

5.4 Characterization using EDS mapping

The EDS mapping was performed on an SEM image of heat treated copper doped titania sample to show the distribution of all the elements present in that sample. Since this sample has Titania to be the main element present in high concentration, it is seen from the red image of Figure 21 that titania element is present everywhere in the sample. The green and blue images show the distribution of copper element and since the doping of copper is 5% with respect to titania it is seen to be in much lesser quantity then titania element. Thus it can be stated that the copper dopant is evenly distributed on the fibers not concentrated in areas. The distribution of oxygen and carbon elements are also shown by the pink and orange images.

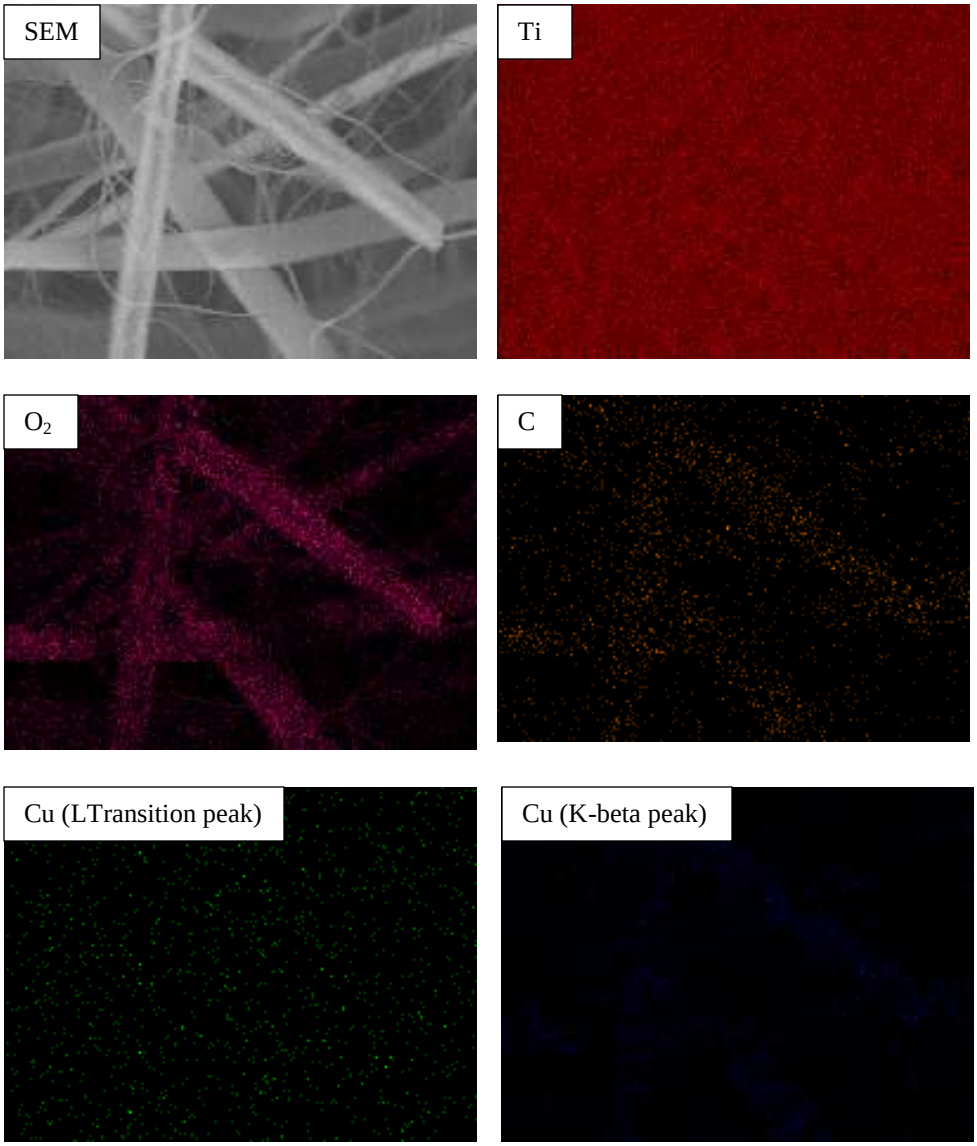

Figure 21: EDS mapping of the annealed copped doped titania showing the distribution of its elements

5.5 Characterization using XRD

It was important to analyze the phases of the photocatalyst prepared since it is said that the anatase phase of titanium dioxide works best as a photocatalyst. For this purpose, the heat treated

samples were studied using the XRD. The XRD results of pure titania photocatalysts annealed at 450^0C are shown below in Figure 22:

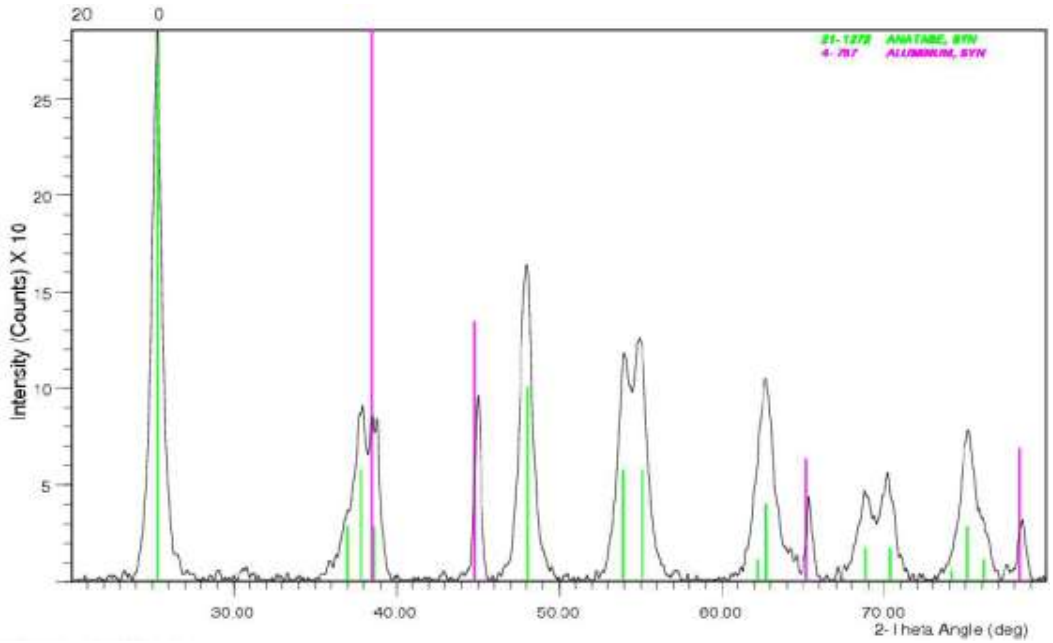

Figure 22: XRD of pure titania annealed at 450^0C for 30 minutes

The XRD above shows that the sample under analysis is completely in the anatase phase, seen by the green peaks. The pink peaks in the graph correspond to aluminum metal which is detected since the sample holder is made of aluminum. Thus, the pure titania photocatalyst synthesized in this work consists of the anatase phase.

Figure 23 below shows the XRD results of copper doped titania fibers annealed at 450^0C

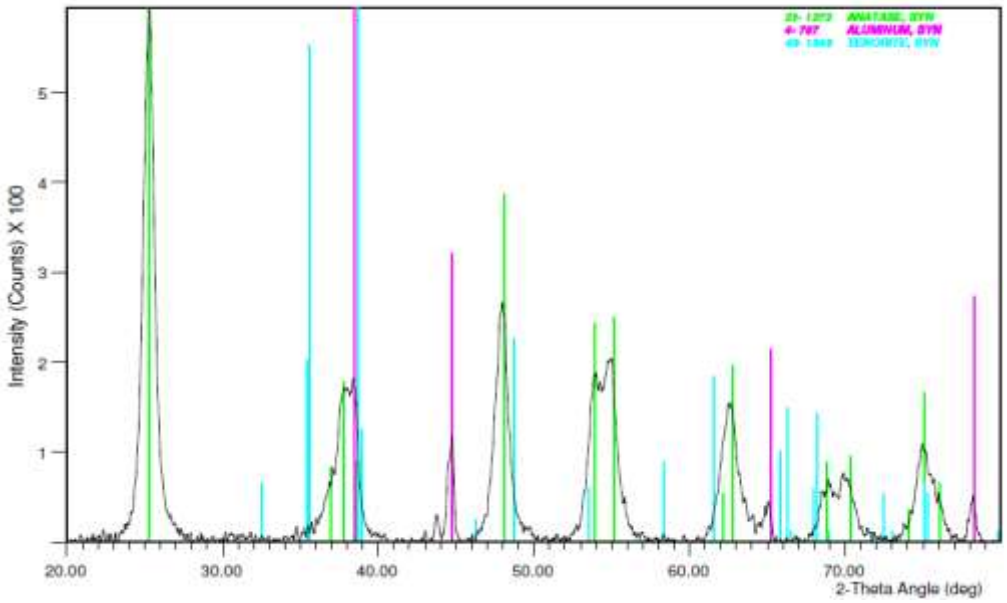

Figure 23: XRD of copper doped titania annealed at 450^{0}C for 30 minutes

Again we see that this catalyst also is made up of the anatase phase of titania (green peaks). Since this sample is the copper doped titania, tenorite peaks (blue peaks) has been shown but since the concentration of copper is very low, this XRD has not detected it. However, the presence of copper is shown in the EDAX results for the same sample. Here again the aluminum of the sample holder has been detected (pinks peaks).

Figure 24 below shows the XRD for copper doped degussa TiO_2 photocatalyst, annealed at 450^{0}C. Since degussa is made up of about 75% anatase and 25% rutile, the XRD shows the same. Here again since copper concentration is very low, it is not detected in this XRD but is shown in the EDAX results. The green lines correspond to the anatase and the pink lines are the rutile phase.

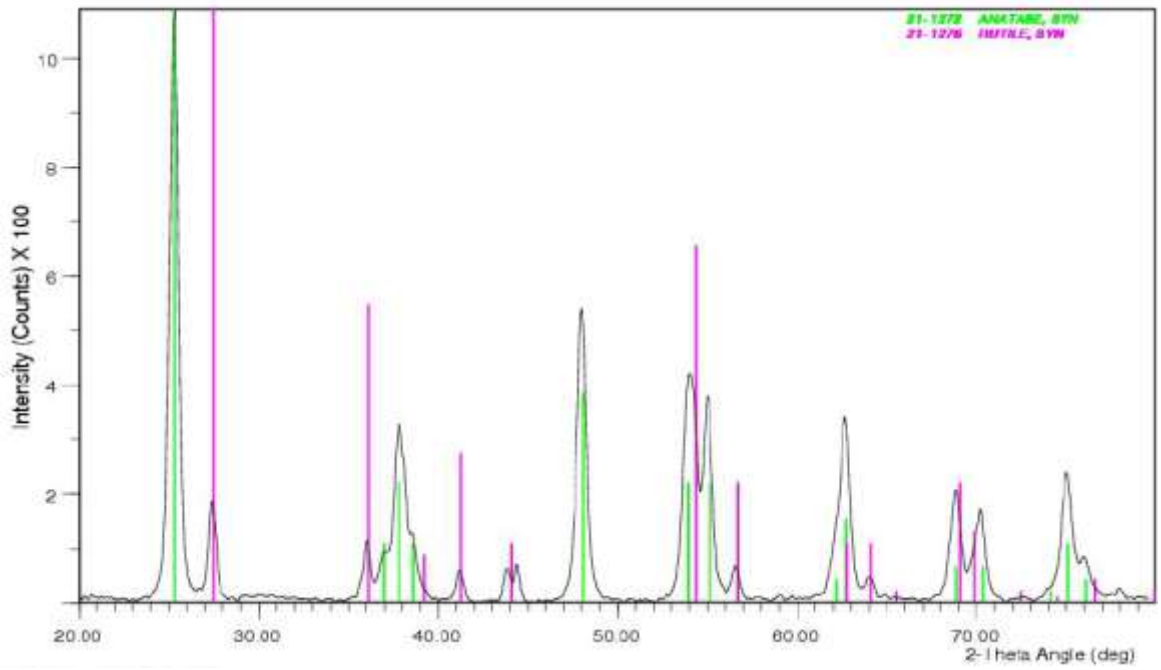

Figure 24: XRD of degussa P25 showing anatase and rutile phases

5.6 Effect of annealing temperature

The temperature chosen to anneal the electrospun samples was 450^0C since the aim was to remove all the polymer from the as-spun material and to synthesize an anatase photocatalyst. Anatase phase of Titania has been reported to have a greater efficiency as a photocatalyst than the rutile phase (Sclafani and Herrmann 1996, Wang and Ying 1999). Anatase phase is generally noted to be formed in the range of 400-500^0C and by further increase in temperature anatase to rutile transition occurs.

To show the anatase to rutile transition, the as-spun pure Titania samples were heat treated at 550^0C for 30 minutes. These samples were then analyzed with the XRD. Figure 25 shows the XRD for this sample which has peaks that correspond to anatase and rutile phase. This is not the case when the sample was heat treated at 450^0C where the XRD showed only anatase peaks as in figure 26.

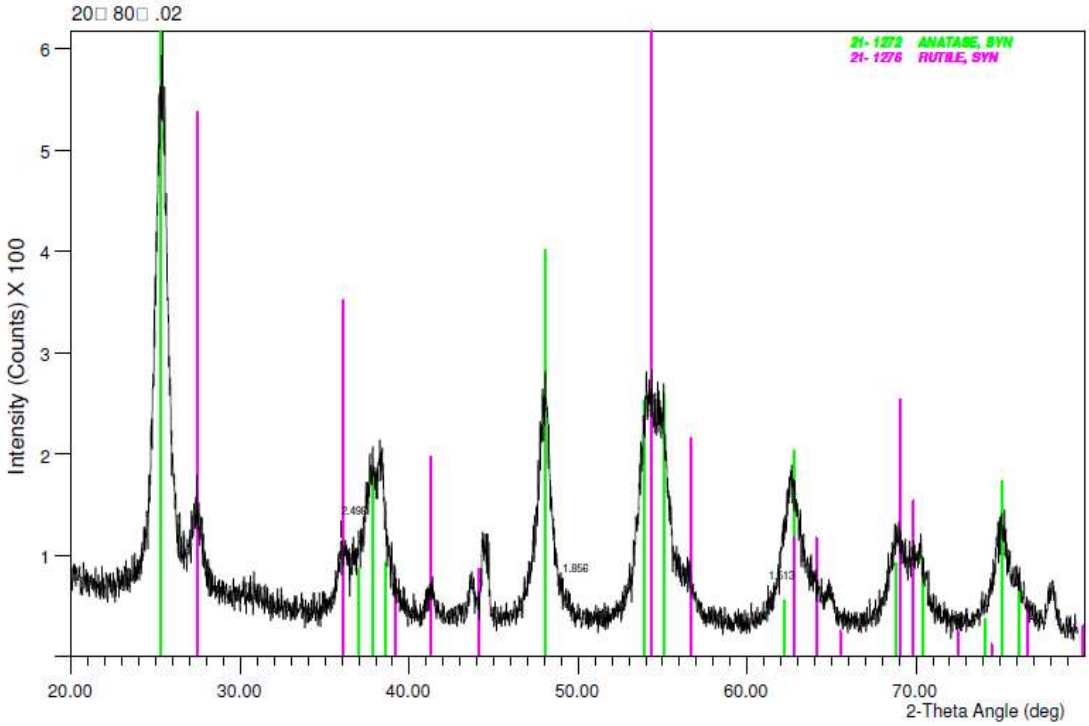

Figure 25: XRD of pure titania annealed at 550^{0}C for 30 minutes

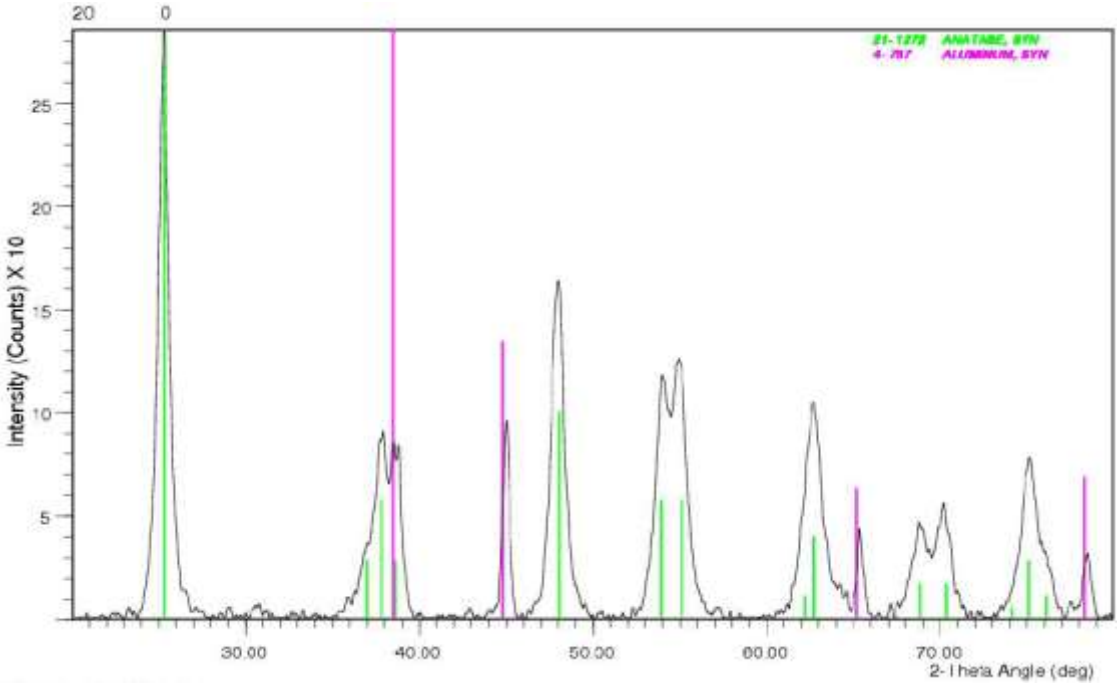

Figure 26: XRD of pure titania annealed at 450^{0}C for 30 minutes

5.7 UV-Vis spectroscopic analysis

The photocatalysts synthesized along with the commercial degussa P25 TiO_2 were tested by checking for the degradation of methylene blue first under UV light and then under Visible Light (by using a 400nm cut off filter). The absorbance value was taken at a wavelength of 665nm for every measurement.

For each test, 0.018g of the catalyst was added to a 4ml, 50ppm solution of methylene blue. This was then kept in the dark for one hour so that the catalyst and the methylene blue establish an adsorption desorption equilibrium. After an hour, an absorbance measurement was taken to record the value for 0 minutes and then the solution was kept directly under UV light or the visible light (by inserting a 400nm cut off filter to the lamp setup) to check for the photo-catalytic effect of the synthesized catalysts and degussa TiO_2, by checking the degradation of methylene blue solution. Four plots, each for a different time have been plotted in the same graph using absorbance values against wavelength. The peak absorbance for all these plots is at 665nm.

5.7.1 Absorbance graphs for UV-light degradation

The Figure 27 below shows the graph of methylene blue solution subjected to degradation under UV light by using the synthesized pure titania photocatalyst. The analysis of this plot shows that the absorbance value was about 1.7 before the UV illumination and gradually decreased and became 0.09 at the end of three hours. The dye degradation percentage calculated at the end of three hours is 94%.

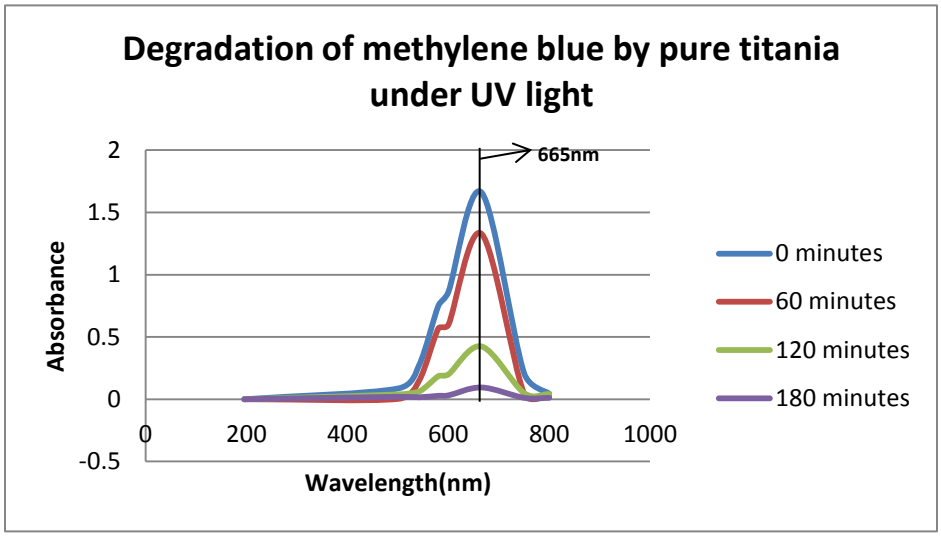

Figure 27: Graph of absorbance versus wavelength (nm) for pure titania under UV light

The Figure 28 shows the degradation of methylene blue dye solution with copper doped titania photocatalyst under UV light illumination. It can be seen that the degradation at 180 minutes is lesser than that for pure titania (Figure 27). The final degradation of the dye in 180 minutes is 82%.

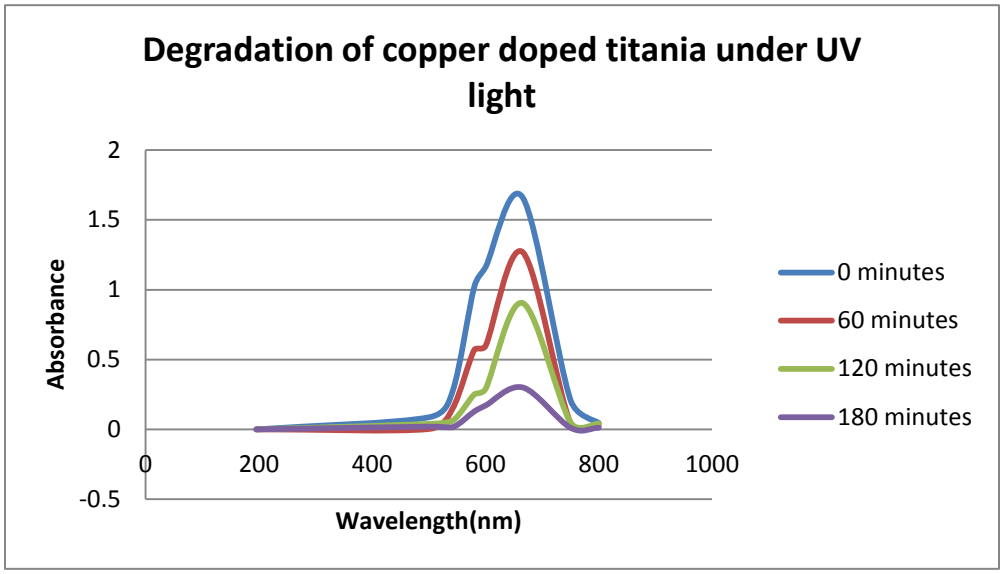

Figure 28: Graph of absorbance versus wavelength (nm) for copper doped titania under UV light

The Figure 29 shows the degradation of methylene blue dye solution with commercial available degussa P25 titanium dioxide under UV light illumination. It can be seen that the degradation at 180 minutes is even lesser than copper doped titania (Figure 28). The final degradation of the dye in 180 minutes is calculated to be 60%

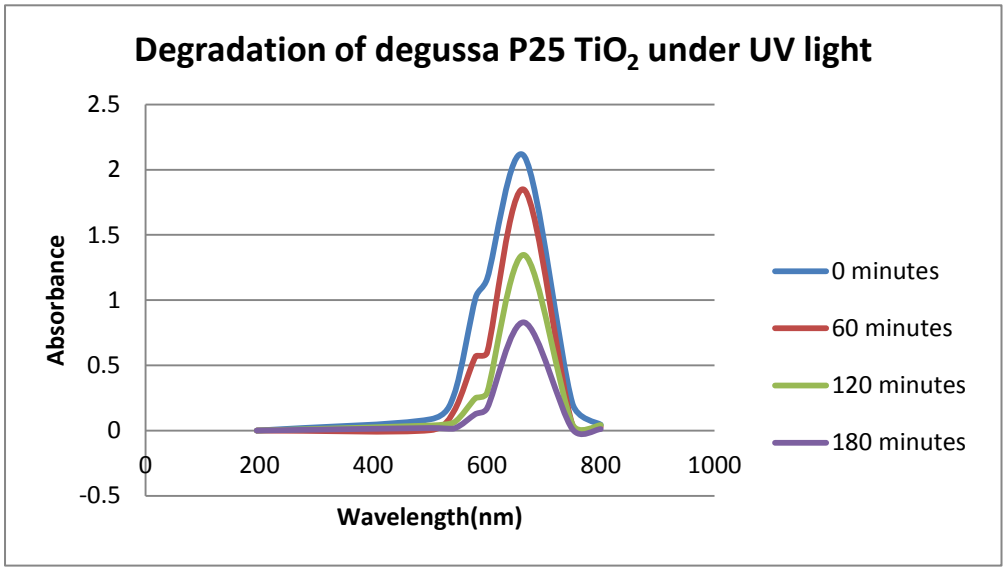

Figure 29: Graph of absorbance versus wavelength (nm) for degussa P25 under UV light

The Figure 30 shows the degradation of methylene blue dye solution with copper doped degussa P25 under UV light illumination. It can be seen that the degradation at 180 minutes is better than commercial degussa (Figure 29). The final degradation of the dye in 180 minutes is calculated to be 78%.

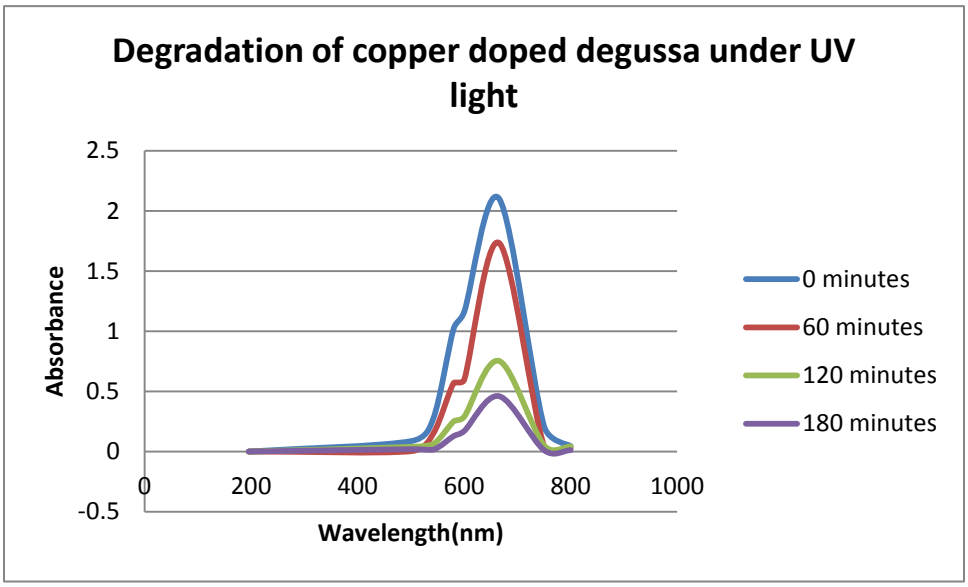

Figure 30: Graph of absorbance versus wavelength (nm) for copper doped degussa under UV light

The Table 3 below displays the degradation percentage for the four catalysts at a time of 180 minutes.

Table 3: Degradation percentage of catalysts under UV light at 180 minutes

	Pure titania nanofibers	**Copper doped Titania nanofibers**	**Degussa P25 TiO_2**	**Copper doped degussa**
Irradiation Time(minutes)	180	180	180	180
Percentage degradation	94%	82%	60%	78%

5.7.2 Absorbance graphs for visible light degradation

For analysis of dye degradation under visible light irradiation, the same procedures used for UV light were followed.

Figure 31 shows the degradation results of methylene blue dye with pure titania photocatalyst under visible light. It can be seen that the absorbance value at the start of the experiment that is at 0 minutes is around 1.8 and in 3 hours of Visible light exposure, the absorbance value has dropped to 1.08. The percentage degradation in 180 minutes is calculated to be 40%.

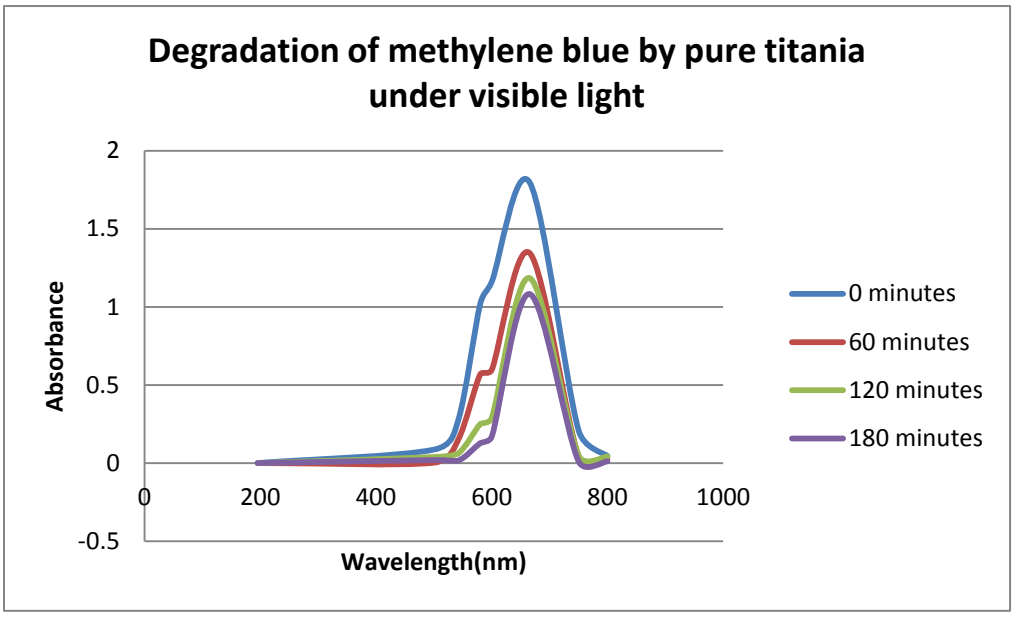

Figure 31: Graph of absorbance versus wavelength (nm) for pure titania under visible light

The Figure 32 shows the degradation of methylene blue dye solution with copper doped titania under visible light illumination. It can be seen that the degradation at 180 minutes has much better results than pure titania photocatalyst (Figure 31). The final degradation of the dye in 180 minutes is calculated to be 97%.

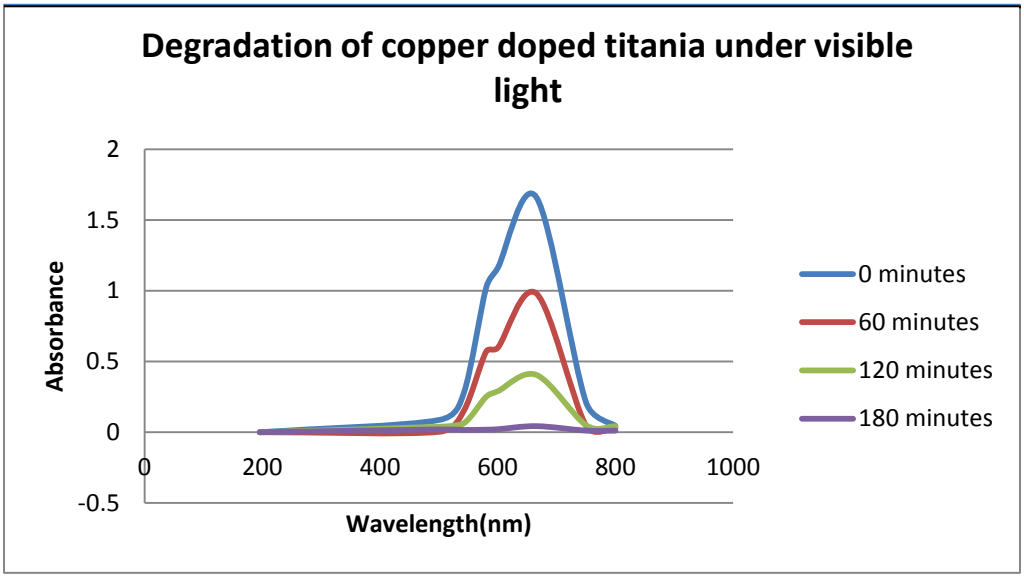

Figure 32: Graph of absorbance versus wavelength (nm) for copper doped titania under visible light

The Figure 33 shows the degradation of methylene blue dye solution with commercial degussa P25 titanium dioxide under visible light illumination. It is studied from the graph that hardly any degradation of the dye has occurred with this catalyst under visible light unlike under UV light degradation where it showed a clear degradation percentage. The dye solution has degraded to only about 11% in 3 hours under visible light.

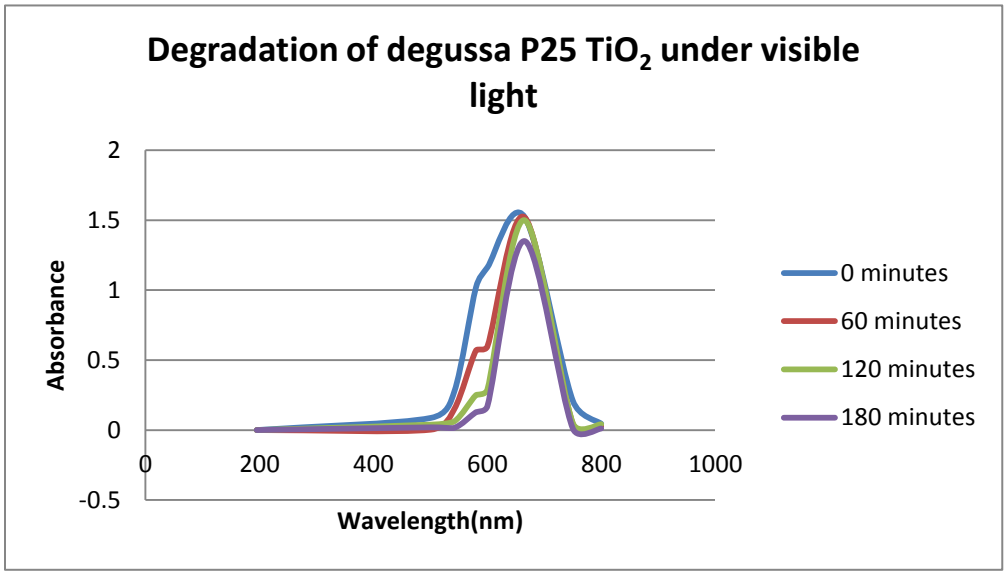

Figure 33: Graph of absorbance versus wavelength (nm) for degussa P25 under visible light

The Figure 34 shows the degradation of methylene blue dye solution with copper doped degussa P25 titanium dioxide under visible light illumination. As seen from the four plots which are obtained at different time intervals, there is no decrease in absorbance value after 180 minutes. The value of absorbance at 0 minutes is 1.37 and after 180 minutes is 1.32. Therefore there has been only 4% degradation.

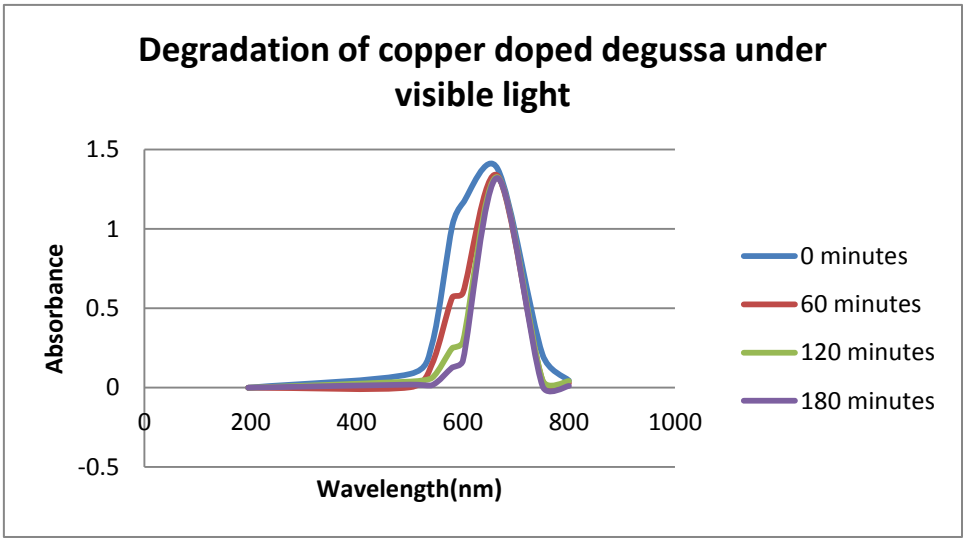

Figure 34: Graph of absorbance versus wavelength (nm) for copper doped degussa P25 under visible light

A table displaying the degradation percentage of all the four catalysts under visible light irradiation at 180 minutes is shown in Table 4 below:

Table 4: Degradation percentage of the four catalysts under visible light at 180mintes

	Pure titania nanofibers	**Copper doped titania nanofibers**	**Degussa P25 TiO_2**	**Copper doped degussa**
Irradiation Time(minutes)	180	180	180	180
Percentage degradation	40%	97%	11%	4%

5.7.3 Comparative analysis of degradation under UV light

In order to get a clearer picture of the degradation for all the four catalysts with respect to each other under UV light, Figure 35 was plotted. The X-axis has the absolute value of absorbance obtained by dividing the absorbance value at time C by the absorbance value at time C_0= 0 minutes. These absolute absorbance values were plotted against time for each catalyst.

Thus the comparative degradation graph under UV light is shown in Figure 35:

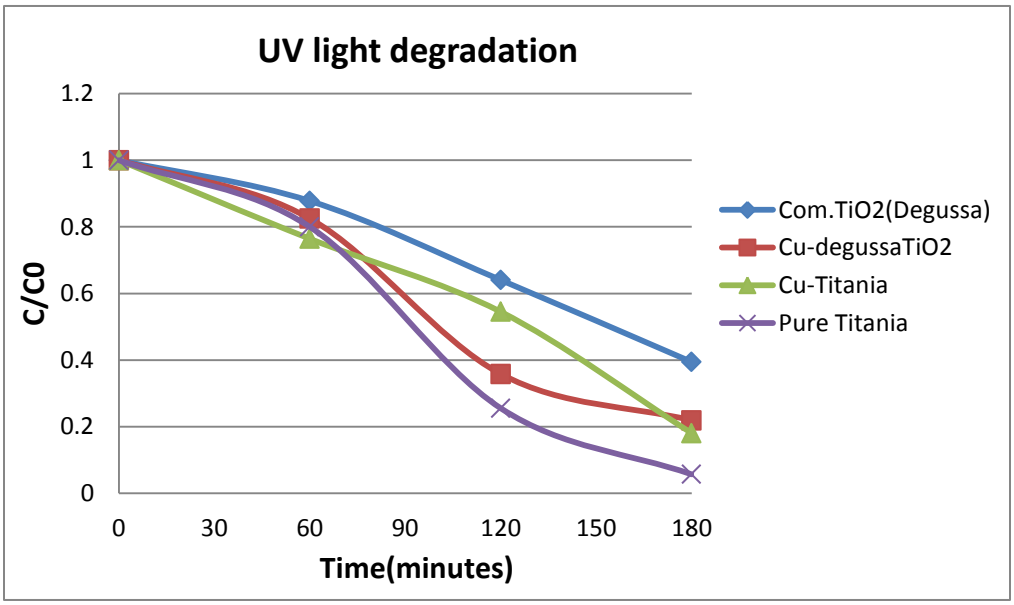

Figure 35: Graph of the degradation of the four catalysts under UV irradiation

5.7.4 Comparative analysis of degradation under visible light

In order to get a clearer picture of the degradation for all the four catalysts with respect to each other under visible light, Figure 36 was plotted. The X-axis has the absolute value of absorbance obtained by dividing the absorbance value at time C by the absorbance value at time C_0= 0 minutes. These absolute absorbance values were plotted against time for each catalyst.

Thus the comparative degradation graph under visible light is shown in Figure 36:

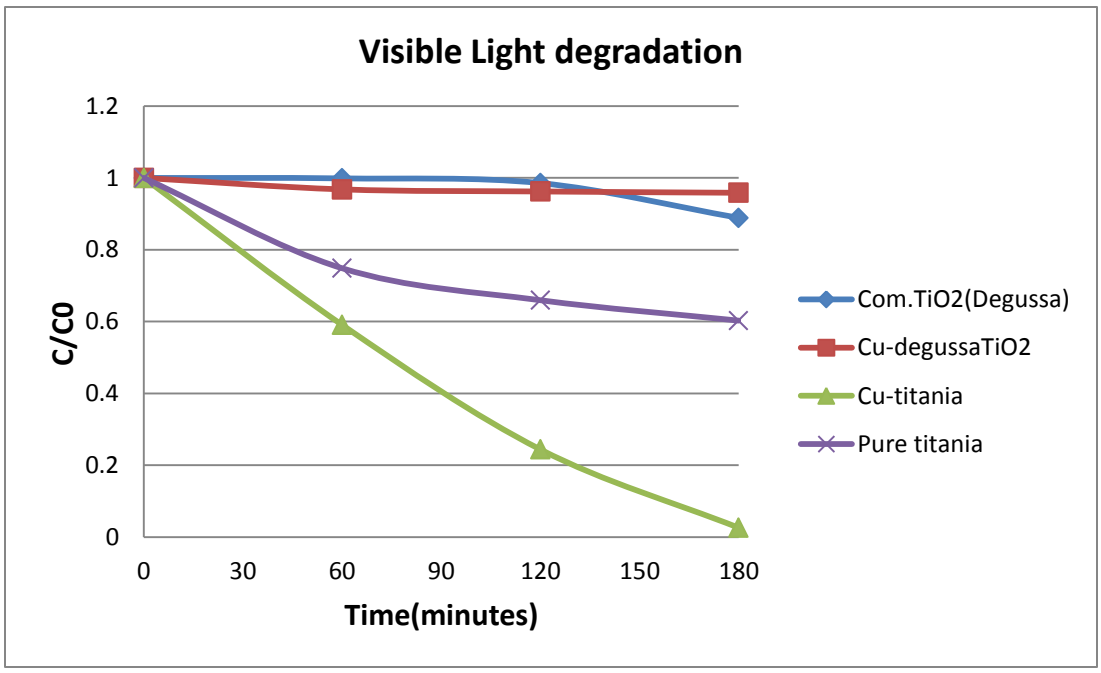

Figure 36: Graph of the degradation of the four catalysts under visible light irradiation

Therefore, from the above graph it is evident that there is a large increase in the degradation percentage (97%) by using copper doped titania photocatalysts upon visible light irradiation.

To the best of my knowledge, there are no reports in the literature on the electrospinning method for copper doped titania photocatalyst except that Lee et al., have very recently(March,2013) prepared copper doped titania photocatalyst synthesized by the electrospinning method but have not studied the visible light degradation in detail (Lee, Bai et al. 2013). It is for the first time that a visible light active copper doped titania having a degradation percentage of 97% has been prepared by the elctrospinning method, tested with methylene blue solution. Thus, it can be said that copper doped titania photocatalysts effective under sunlight have been synthesized with a high degradation rate.

CHAPTER 6: CONCLUSIONS

Thus, the photocatalytic activities of all the synthesized catalysts have been demonstrated under UV light and under visible light. Characterization methods were used to understand and study the morphology of the nanocomposites. The UV-Vis spectroscopy results display that the degradation of MB solution was the best with the synthesized pure titania photocatalysts showing 94% degradation when irradiated under UV light while the commercial titanium dioxide (degussa P25) showed only 60% degradation for the same irradiation time.

A strongly effective visible light photocatalyst was synthesized in this work with the UV-Vis spectroscopy results exhibiting 97% degradation under visible light by using the copper doped titania photocatalyst. Under the same conditions, the commercial titanium dioxide (degussa P25) showed a weak 11% degradation. Thus, the theory behind the doping of titania with copper to produce a better catalyst goes in hand with the experimental results obtained in this work.

Therefore factors such as concentration of dopant, nanofiber morphology and the anatase phase of crystals along with doping which was incorporated to reduce the bang gap energy in order to accelerate the formation of holes that combine with water to form –OH radicals, have all contributed to producing an efficient copper doped titania photocatalyst highly active under the visible light spectrum having a great potential in wastewater treatment.

Our future work would aim at increasing the concentration of dopant, trying to synthesize single crystal nanofibers that are reusable and thus believed to make effective photocatalysts.

References

Abe, R., K. Sayama and H. Arakawa (2004). "Dye-sensitized photocatalysts for efficient hydrogen production from aqueous I- solution under visible light irradiation." Journal of Photochemistry and Photobiology a-Chemistry **166**(1-3): 115-122.

Adomaviciute, E. and R. Milasius (2007). "The influence of applied voltage on poly(vinyl alcohol) (PVA) nanofibre diameter." Fibres & Textiles in Eastern Europe **15**(5-6): 69-72.

Akyol, A. and M. Bayramoglu (2010). "Performance comparison of ZnO photocatalyst in various reactor systems." Journal of Chemical Technology and Biotechnology **85**(11): 1455-1462.

Allegre, C., P. Moulin, M. Maisseu and F. Charbit (2006). "Treatment and reuse of reactive dyeing effluents." Journal of Membrane Science **269**(1-2): 15-34.

Aramendia, M. A., J. C. Colmenares, A. Marinas, J. M. Marinas, J. M. Moreno, J. A. Navio and F. J. Urbano (2007). "Effect of the redox treatment of Pt/TiO2 system on its photocatalytic behaviour in the gas phase selective photooxidation of propan-2-ol." Catalysis Today **128**(3-4): 235-244.

Arana, J., J. Martınez Nieto, J. Herrera Melián, J. Dona Rodrıguez, O. Gonzalez Dıaz, J. Pérez Pena, O. Bergasa, C. Alvarez and J. Méndez (2004). "Photocatalytic degradation of formaldehyde containing wastewater from veterinarian laboratories." Chemosphere **55**(6): 893-904.

Arinstein, A. and E. Zussman (2007). "Postprocesses in tubular electrospun nanofibers." Physical Review E **76**(5).

Bacsa, R., J. Kiwi, T. Ohno, P. Albers and V. Nadtochenko (2005). "Preparation, testing and characterization of doped TiO2 active in the peroxidation of biomolecules under visible light." Journal of Physical Chemistry B **109**(12): 5994-6003.

Bauer, C., G. Boschloo, E. Mukhtar and A. Hagfeldt (2002). "Interfacial electron-transfer dynamics in Ru(tcterpy)(NCS)(3)-sensitized TiO2 nanocrystalline solar cells." Journal of Physical Chemistry B **106**(49): 12693-12704.

Baumgarten, P. K. (1971). "Electrostatic spinning of acrylic microfibers." Journal of colloid and interface science **36**(1): 71-79.

Bensaha, R. and H. Bensouyad (2012). Synthesis, Characterization and Properties of Zirconium Oxide (ZrO2)-Doped Titanium Oxide (TiO2) Thin Films Obtained via Sol-Gel Process.

Bhatkhande, D. S., S. P. Kamble, S. B. Sawant and V. G. Pangarkar (2004). "Photocatalytic and photochemical degradation of nitrobenzene using artificial ultraviolet light." Chemical Engineering Journal **102**(3): 283-290.

Buchko, C. J., L. C. Chen, Y. Shen and D. C. Martin (1999). "Processing and microstructural characterization of porous biocompatible protein polymer thin films." Polymer **40**(26): 7397-7407.

Burger, C., B. S. Hsiao and B. Chu (2006). "Nanofibrous materials and their applications." Annu. Rev. Mater. Res. **36**: 333-368.

Carp, O., C. L. Huisman and A. Reller (2004). "Photoinduced reactivity of titanium dioxide." Progress in Solid State Chemistry **32**(1-2): 33-177.

Casper, C. L., J. S. Stephens, N. G. Tassi, D. B. Chase and J. F. Rabolt (2004). "Controlling surface morphology of electrospun polystyrene fibers: Effect of humidity and molecular weight in the electrospinning process." Macromolecules **37**(2): 573-578.

Chandrasekhar, S. and P. N. Pramada (2006). "Rice husk ash as an adsorbent for methylene blue-effect of ashing temperature." Adsorption-Journal of the International Adsorption Society **12**(1): 27-43.

Chen, L. C., C. M. Huang and F. R. Tsai (2007). "Characterization and photocatalytic activity of K+-doped TiO2 photocatalysts." Journal of Molecular Catalysis a-Chemical **265**(1-2): 133-140.

Chew, S. Y., Y. Wen, Y. Dzenis and K. W. Leong (2006). "The role of electrospinning in the emerging field of nanomedicine." Current Pharmaceutical Design **12**(36): 4751-4770.
Childs, R. F. and M. E. Hagar (1980). "Photo-Isomerization and Thermal-Isomerization of Some 1-Methoxyallyl Cations." Canadian Journal of Chemistry-Revue Canadienne De Chimie **58**(17): 1788-1794.
Choi, S. K., S. Kim, S. K. Lim and H. Park (2010). "Photocatalytic Comparison of TiO2 Nanoparticles and Electrospun TiO2 Nanofibers: Effects of Mesoporosity and Interparticle Charge Transfer." Journal of Physical Chemistry C **114**(39): 16475-16480.
Choi, W. Y., A. Termin and M. R. Hoffmann (1994). "Effects of Metal-Ion Dopants on the Photocatalytic Reactivity of Quantum-Sized Tio2 Particles." Angewandte Chemie-International Edition in English **33**(10): 1091-1092.
Chong, E. J., T. T. Phan, I. J. Lim, Y. Z. Zhang, B. H. Bay, S. Ramakrishna and C. T. Lim (2007). "Evaluation of electrospun PCL/gelatin nanofibrous scaffold for wound healing and layered dermal reconstitution." Acta Biomaterialia **3**(3): 321-330.
Chong, M. N., B. Jin, C. W. K. Chow and C. Saint (2010). "Recent developments in photocatalytic water treatment technology: A review." Water Research **44**(10): 2997-3027.
Chun, H., W. Yizhong and T. Hongxiao (2000). "Destruction of phenol aqueous solution by photocatalysis or direct photolysis." Chemosphere **41**(8): 1205-1209.
Colmenares, J., M. Aramendia, A. Marinas, J. Marinas and F. Urbano (2006). "Synthesis, characterization and photocatalytic activity of different metal-doped titania systems." Applied Catalysis A: General **306**: 120-127.
Colmenares, J. C., R. Luque, J. M. Campelo, F. Colmenares, Z. Karpinski and A. A. Romero (2009). "Nanostructured Photocatalysts and Their Applications in the Photocatalytic Transformation of Lignocellulosic Biomass: An Overview." Materials **2**(4): 2228-2258.
Colombo, D. P. and R. M. Bowman (1996). "Does interfacial charge transfer compete with charge carrier recombination? A femtosecond diffuse reflectance investigation of TiO2 nanoparticles." Journal of Physical Chemistry **100**(47): 18445-18449.
Curco, D., J. Gimenez, A. Addardak, S. Cervera-March and S. Esplugas (2002). "Effects of radiation absorption and catalyst concentration on the photocatalytic degradation of pollutants." Catalysis Today **76**(2-4): 177-188.
Das, K., S. Bose and A. Bandyopadhyay (2009). "TiO2 nanotubes on Ti: Influence of nanoscale morphology on bone cell-materials interaction." Journal of Biomedical Materials Research Part A **90A**(1): 225-237.
Deitzel, J., W. Kosik, S. McKnight, N. Beck Tan, J. DeSimone and S. Crette (2002). "Electrospinning of polymer nanofibers with specific surface chemistry." Polymer **43**(3): 1025-1029.
Deitzel, J. M., J. Kleinmeyer, D. Harris and N. C. B. Tan (2001). "The effect of processing variables on the morphology of electrospun nanofibers and textiles." Polymer **42**(1): 261-272.
Demir, M. M., I. Yilgor, E. Yilgor and B. Erman (2002). "Electrospinning of polyurethane fibers." Polymer **43**(11): 3303-3309.
Diebold, U. (2003). "The surface science of titanium dioxide." Surface Science Reports **48**(5-8): 53-229.
Ding, B., H. Y. Kim, S. C. Lee, C. L. Shao, D. R. Lee, S. J. Park, G. B. Kwag and K. J. Choi (2002). "Preparation and characterization of a nanoscale poly(vinyl alcohol) fiber aggregate produced by an electrospinning method." Journal of Polymer Science Part B-Polymer Physics **40**(13): 1261-1268.
Ding, H. M., H. Sun and Y. K. Shan (2005). "Preparation and characterization of mesoporous SBA-15 supported dye-sensitized TiO2 photocatalyst." Journal of Photochemistry and Photobiology a-Chemistry **169**(1): 101-107.
Doshi, J. and D. H. Reneker (1995). "Electrospinning process and applications of electrospun fibers." Journal of electrostatics **35**(2): 151-160.

El Qada, E. N., S. J. Allen and G. M. Walker (2006). "Adsorption of Methylene Blue onto activated carbon produced from steam activated bituminous coal: A study of equilibrium adsorption isotherm." Chemical Engineering Journal **124**(1-3): 103-110.
Fong, H., I. Chun and D. Reneker (1999). "Beaded nanofibers formed during electrospinning." Polymer **40**(16): 4585-4592.
Fong, H. and D. H. Reneker (1999). "Elastomeric nanofibers of styrene-butadiene-styrene triblock copolymer." Journal of Polymer Science Part B-Polymer Physics **37**(24): 3488-3493.
Friesen, D. A., L. Morello, J. V. Headley and C. H. Langford (2000). "Factors influencing relative efficiency in photo-oxidations of organic molecules by Cs(3)PW(12)O(40) and TiO(2) colloidal photocatalysts." Journal of Photochemistry and Photobiology a-Chemistry **133**(3): 213-220.
Fu, G., P. S. Vary and C.-T. Lin (2005). "Anatase TiO2 nanocomposites for antimicrobial coatings." The Journal of Physical Chemistry B **109**(18): 8889-8898.
Fujishima, A., T. N. Rao and D. A. Tryk (2000). "TiO(2) photocatalysts and diamond electrodes." Electrochimica Acta **45**(28): 4683-4690.
Gaya, U. I. and A. H. Abdullah (2008). "Heterogeneous photocatalytic degradation of organic contaminants over titanium dioxide: A review of fundamentals, progress and problems." Journal of Photochemistry and Photobiology C-Photochemistry Reviews **9**(1): 1-12.
Ge, L. and M. X. Xu (2006). "Influences of the Pd doping on the visible light photocatalytic activities of InVO4-TiO2 thin films." Materials Science and Engineering B-Solid State Materials for Advanced Technology **131**(1-3): 222-229.
Geng, X. Y., O. H. Kwon and J. H. Jang (2005). "Electrospinning of chitosan dissolved in concentrated acetic acid solution." Biomaterials **26**(27): 5427-5432.
Gillman, P. K. (2006). "Methylene blue implicated in potentially fatal serotonin toxicity." Anaesthesia **61**(10): 1013-1014.
Gillman, P. K. (2008). "Methylene blue is a potent monoamine oxidase inhibitor." Canadian Journal of Anaesthesia-Journal Canadien D Anesthesie **55**(5): 311-312.
Gong, D., C. A. Grimes, O. K. Varghese, W. C. Hu, R. S. Singh, Z. Chen and E. C. Dickey (2001). "Titanium oxide nanotube arrays prepared by anodic oxidation." Journal of Materials Research **16**(12): 3331-3334.
Gupta, P., C. Elkins, T. E. Long and G. L. Wilkes (2005). "Electrospinning of linear homopolymers of poly(methyl methacrylate): exploring relationships between fiber formation, viscosity, molecular weight and concentration in a good solvent." Polymer **46**(13): 4799-4810.
Haghi, A. K. and M. Akbari (2007). "Trends in electrospinning of natural nanofibers." Physica Status Solidi a-Applications and Materials Science **204**(6): 1830-1834.
Haque, M. and M. Muneer (2007). "Photodegradation of norfloxacin in aqueous suspensions of titanium dioxide." Journal of Hazardous materials **145**(1): 51-57.
Hashimoto, K., H. Irie and A. Fujishima (2005). "TiO2 photocatalysis: A historical overview and future prospects." Japanese Journal of Applied Physics Part 1-Regular Papers Brief Communications & Review Papers **44**(12): 8269-8285.
He, J. J., J. C. Zhao, T. Shen, H. Hidaka and N. Serpone (1997). "Photosensitization of colloidal titania particles by electron injection from an excited organic dye-antennae function." Journal of Physical Chemistry B **101**(44): 9027-9034.
Helaili, N., Y. Bessekhouad, A. Bouguelia and M. Trari (2009). "Visible light degradation of Orange II using xCu(y)O(z)/TiO2 heterojunctions." Journal of Hazardous Materials **168**(1): 484-492.
Heller, A. (1995). "Chemistry and applications of photocatalytic oxidation of thin organic films." Accounts of Chemical Research **28**(12): 503-508.
Hohman, M. M., M. Shin, G. Rutledge and M. P. Brenner (2001). "Electrospinning and electrically forced jets. II. Applications." Physics of Fluids **13**(8): 2221-2236.

Houas, A., H. Lachheb, M. Ksibi, E. Elaloui, C. Guillard and J.-M. Herrmann (2001). "Photocatalytic degradation pathway of methylene blue in water." Applied Catalysis B: Environmental **31**(2): 145-157.
Huang, L., K. Nagapudi, R. P. Apkarian and E. L. Chaikof (2001). "Engineered collagen-PEO nanofibers and fabrics." Journal of Biomaterials Science-Polymer Edition **12**(9): 979-993.
Huang, Z. M., Y. Z. Zhang, M. Kotaki and S. Ramakrishna (2003). "A review on polymer nanofibers by electrospinning and their applications in nanocomposites." Composites Science and Technology **63**(15): 2223-2253.
Hufschmidt, D., L. Liu, V. Selzer and D. Bahnemann (2004). "Photocatalytic water treatment: fundamental knowledge required for its practical application." Water Science and Technology **49**(4): 135-140.
Hull, A. (1919). "A new method of chemical analysis." Journal of the American Chemical Society **41**(8): 1168-1175.
Irmak, S., E. Kusvuran and O. Erbatur (2004). "Degradation of 4-chloro-2-methylphenol in aqueous solution by UV irradiation in the presence of titanium dioxide." Applied Catalysis B-Environmental **54**(2): 85-91.
Jalili, R., S. A. Hosseini and M. Morshed (2005). "The effects of operating parameters on the morphology of electrospun polyacrilonitrile nanofibres." Iranian Polymer Journal **14**(12): 1074-1081.
Jian-xiao, L., C. Ying, X. Guo-hong, Z. Ling-yun and W. Su-fen (2011). "Decoloration of methylene blue simulated wastewater using a UV-H< sub> 2</sub> O< sub> 2</sub> combined system." Journal of Water Reuse and Desalination **1**(1): 45-51.
Jiang, H. L., D. F. Fang, B. S. Hsiao, B. Chu and W. L. Chen (2004). "Optimization and characterization of dextran membranes prepared by electrospinning." Biomacromolecules **5**(2): 326-333.
Jin, Z. L., X. J. Zhang, Y. X. Li, S. B. Li and G. X. Lu (2007). "5.1% Apparent quantum efficiency for stable hydrogen generation over eosin-sensitized CuO/TiO2 photocatalyst under visible light irradiation." Catalysis Communications **8**(8): 1267-1273.
Jin, Z. L., X. J. Zhang, G. X. Lu and S. B. Li (2006). "Improved quantum yield for photocatalytic hydrogen generation under visible light irradiation over eosin sensitized TiO2 - Investigation of different noble metal loading." Journal of Molecular Catalysis a-Chemical **259**(1-2): 275-280.
Jun, Z., H. Q. Hou, A. Schaper, J. H. Wendorff and A. Greiner (2003). "Poly-L-lactide nanofibers by electrospinning - Influence of solution viscosity and electrical conductivity on fiber diameter and fiber morphology." E-Polymers.
Kanjwal, M. A., N. A. M. Barakat, F. A. Sheikh, M. S. Khil and H. Y. Kim (2010). "Functionalization of Electrospun Titanium Oxide Nanofibers with Silver Nanoparticles: Strongly Effective Photocatalyst." International Journal of Applied Ceramic Technology **7**: E54-E63.
Karakitsou, K. E. and X. E. Verykios (1993). "Effects of Altervalent Cation Doping of Tio2 on Its Performance as a Photocatalyst for Water Cleavage." Journal of Physical Chemistry **97**(6): 1184-1189.
Karunakaran, C. and S. Senthilvelan (2005). "Photooxidation of aniline on alumina with sunlight and artificial UV light." Catalysis Communications **6**(2): 159-165.
Ki, C. S., D. H. Baek, K. D. Gang, K. H. Lee, I. C. Um and Y. H. Park (2005). "Characterization of gelatin nanofiber prepared from gelatin-formic acid solution." Polymer **46**(14): 5094-5102.
Kidoaki, S., I. K. Kwon and T. Matsuda (2005). "Mesoscopic spatial designs of nano- and microfiber meshes for tissue-engineering matrix and scaffold based on newly devised multilayering and mixing electrospinning techniques." Biomaterials **26**(1): 37-46.
Kim, H., S. Lee, Y. Han and J. Park (2005). "Preparation of dip-coated TiO2 photocatalyst on ceramic foam pellets." Journal of Materials Science **40**(19): 5295-5298.
Kim, K. H., L. Jeong, H. N. Park, S. Y. Shin, W. H. Park, S. C. Lee, T. I. Kim, Y. J. Park, Y. J. Seol, Y. M. Lee, Y. Ku, I. C. Rhyu, S. B. Han and C. P. Chung (2005). "Biological efficacy of silk fibroin nanofiber membranes for guided bone regeneration." Journal of Biotechnology **120**(3): 327-339.

Kisch, H. and W. Macyk (2002). "Visible-light photocatalysis by modified titania." Chemphyschem **3**(5): 399-+.
Kitano, M., M. Matsuoka, M. Ueshima and M. Anpo (2007). "Recent developments in titanium oxide-based photocatalysts." Applied Catalysis a-General **325**(1): 1-14.
Kogo, K., H. Yoneyama and H. Tamura (1980). "Photocatalytic Oxidation of Cyanide on Platinized Tio2." Journal of Physical Chemistry **84**(13): 1705-1710.
Konstantinou, I. K. and T. A. Albanis (2004). "TiO2-assisted photocatalytic degradation of azo dyes in aqueous solution: kinetic and mechanistic investigations - A review." Applied Catalysis B-Environmental **49**(1): 1-14.
Kosmulski, M. (2004). "pH-dependent surface charging and points of zero charge II. Update." Journal of colloid and interface science **275**(1): 214-224.
Krysa, J., M. Keppert, J. Jirkovsky, V. Stengl and J. Subrt (2004). "The effect of thermal treatment on the properties of TiO(2) photocatalyst." Materials Chemistry and Physics **86**(2-3): 333-339.
Kryukova, G. N., G. A. Zenkovets, A. A. Shutilov, M. Wilde, K. Gunther, D. Fassler and K. Richter (2007). "Structural peculiarities of TiO2 and Pt/TiO2 catalysts for the photocatalytic oxidation of aqueous solution of Acid Orange 7 Dye upon ultraviolet light." Applied Catalysis B-Environmental **71**(3-4): 169-176.
Kudo, A. and Y. Miseki (2009). "Heterogeneous photocatalyst materials for water splitting." Chemical Society Reviews **38**(1): 253-278.
Kwon, C. H., H. Shin, J. H. Kim, W. S. Choi and K. H. Yoon (2004). "Degradation of methylene blue via photocatalysis of titanium dioxide." Materials Chemistry and Physics **86**(1): 78-82.
Lakshmi, S., R. Renganathan and S. Fujita (1995). "Study on TiO2-mediated photocatalytic degradation of methylene blue." Journal of Photochemistry and Photobiology A: Chemistry **88**(2–3): 163-167.
Larrondo, L. and R. S. J. Manley (1981). "Electrostatic Fiber Spinning from Polymer Melts .1. Experimental-Observations on Fiber Formation and Properties." Journal of Polymer Science Part B-Polymer Physics **19**(6): 909-920.
Lawless, D., N. Serpone and D. Meisel (1991). "Role of Oh. Radicals and Trapped Holes in Photocatalysis - a Pulse-Radiolysis Study." Journal of Physical Chemistry **95**(13): 5166-5170.
Leary, R. and A. Westwood (2011). "Carbonaceous nanomaterials for the enhancement of TiO2 photocatalysis." Carbon **49**(3): 741-772.
Lee, J. S., K. H. Choi, H. Do Ghim, S. S. Kim, D. H. Chun, H. Y. Kim and W. S. Lyoo (2004). "Role of molecular weight of atactic poly(vinyl alcohol) (PVA) in the structure and properties of PVA nanofabric prepared by electrospinning." Journal of Applied Polymer Science **93**(4): 1638-1646.
Lee, S. K., S. McIntyre and A. Mills (2004). "Visible illustration of the direct, lateral and remote photocatalytic destruction of soot by titania." Journal of Photochemistry and Photobiology a-Chemistry **162**(1): 203-206.
Lee, S. S., H. Bai, Z. Liu and D. D. Sun (2013). "Novel-Structured Electrospun TiO< sub> 2</sub>/CuO Composite Nanofibers for High Efficient Photocatalytic Cogeneration of Clean Water and Energy from Dye Wastewater." Water research.
Li, Q., D. Sun and H. Kim (2011). "Fabrication of porous TiO2 nanofiber and its photocatalytic activity." Materials Research Bulletin **46**(11): 2094-2099.
Li, Y., W. N. Wang, Z. L. Zhan, M. H. Woo, C. Y. Wu and P. Biswas (2010). "Photocatalytic reduction of CO2 with H2O on mesoporous silica supported Cu/TiO2 catalysts." Applied Catalysis B-Environmental **100**(1-2): 386-392.
Lin, X. P., F. Q. Huang, W. D. Wang and K. L. Zhang (2006). "A novel photocatalyst BiSbO< sub> 4</sub> for degradation of methylene blue." Applied Catalysis A: General **307**(2): 257-262.

Lin, Y. J., S. L. Tseng, W. J. Huang and W. J. Wu (2006). "Enhanced photocatalysis of pentachlorophenol by metal-modified titanium(IV) oxide." Journal of Environmental Science and Health Part B-Pesticides Food Contaminants and Agricultural Wastes **41**(7): 1143-1158.
Ling, C. M., A. R. Mohamed and S. Bhatia (2004). "Performance of photocatalytic reactors using immobilized TiO< sub> 2</sub> film for the degradation of phenol and methylene blue dye present in water stream." Chemosphere **57**(7): 547-554.
Maira, A. J., K. L. Yeung, J. Soria, J. M. Coronado, C. Belver and C. Y. Lee (2001). "Gas-phase photo-oxidation of toluene using nanometer-size TiO2 catalysts." Applied Catalysis B-Environmental **29**(4): 327-336.
Mansilla, H., C. Bravo, R. Ferreyra, M. Litter, W. Jardim, C. Lizama, J. Freer and J. Fernandez (2006). "Photocatalytic EDTA degradation on suspended and immobilized TiO< sub> 2</sub>." Journal of Photochemistry and Photobiology A: Chemistry **181**(2): 188-194.
Matsuda, S., H. Hatano and A. Tsutsumi (2001). "Ultrafine particle fluidization and its application to photocatalytic NOx treatment." Chemical Engineering Journal **82**(1-3): 183-188.
McKee, M. G., G. L. Wilkes, R. H. Colby and T. E. Long (2004). "Correlations of solution rheology with electrospun fiber formation of linear and branched polyesters." Macromolecules **37**(5): 1760-1767.
Megelski, S., J. S. Stephens, D. B. Chase and J. F. Rabolt (2002). "Micro- and nanostructured surface morphology on electrospun polymer fibers." Macromolecules **35**(22): 8456-8466.
Meissner, P. E., G. Mandi, B. Coulibaly, S. Witte, T. Tapsoba, U. Mansmann, J. Rengelshausen, W. Schiek, A. Jahn and I. Walter-Sack (2006). "Methylene blue for malaria in Africa: results from a dose-finding study in combination with chloroquine." Malaria Journal **5**(1): 84.
Meng, X., D. W. Shin, S. M. Yu, J. H. Jung, H. I. Kim, H. M. Lee, Y. H. Han, V. Bhoraskar and J. B. Yoo (2011). "Growth of hierarchical TiO2 nanostructures on anatase nanofibers and their application in photocatalytic activity." Crystengcomm **13**(8): 3021-3029.
Mills, A., C. Hill and P. K. J. Robertson (2012). "Overview of the current ISO tests for photocatalytic materials." Journal of Photochemistry and Photobiology a-Chemistry **237**: 7-23.
Mit-uppatham, C., M. Nithitanakul and P. Supaphol (2004). "Ultrafine Electrospun Polyamide-6 Fibers: Effect of Solution Conditions on Morphology and Average Fiber Diameter." Macromolecular Chemistry and Physics **205**(17): 2327-2338.
Mohammadi, M. R., M. C. Cordero-Cabrera, D. J. Fray and A. Ghorbani (2006). "Preparation of high surface area titania (TiO2)films and powders using particulate sol-gel route aided by polymeric fugitive agents." Sensors and Actuators B-Chemical **120**(1): 86-95.
Muszkat, L., L. Feigelson, L. Bir and K. A. Muszkat (2002). "Photocatalytic degradation of pesticides and bio-molecules in water." Pest Management Science **58**(11): 1143-1148.
Okato, T., T. Sakano and M. Obara (2005). "Suppression of photocatalytic efficiency in highly N-doped anatase films." Physical Review B **72**(11).
Owen, T. (1996). Fundamentals of modern UV-visible spectroscopy: A primer, Hewlett-Packard.
Palmisano, G., M. Addamo, V. Augugliaro, T. Caronna, A. Di Paola, E. G. Lopez, V. Loddo, G. Marci, L. Palmisano and M. Schiavello (2007). "Selectivity of hydroxyl radical in the partial oxidation of aromatic compounds in heterogeneous photocatalysis." Catalysis Today **122**(1-2): 118-127.
Pan, J. H., H. Q. Dou, Z. G. Xiong, C. Xu, J. Z. Ma and X. S. Zhao (2010). "Porous photocatalysts for advanced water purifications." Journal of Materials Chemistry **20**(22): 4512-4528.
Park, H. S., D. H. Kim, S. J. Kim and K. S. Lee (2006). "The photocatalytic activity of 2.5 wt% Cu-doped TiO2 nano powders synthesized by mechanical alloying." Journal of Alloys and Compounds **415**(1-2): 51-55.
Park, J. Y., C. Lee, K. W. Jung and D. Jung (2009). "Structure Related Photocatalytic Properties of TiO2." Bulletin of the Korean Chemical Society **30**(2): 402-404.

Pelizzetti, E., C. Minero, V. Maurino, A. Sclafani, H. Hidaka and N. Serpone (1989). "Photocatalytic Degradation of Nonylphenol Ethoxylated Surfactants." Environmental Science & Technology **23**(11): 1380-1385.
Perciasepe, B., D. McLerran, W. W. Stelle Jr, R. Blank, R. Thorson and P. Region (2013). "Re: Supplemental 60-Day Notice of Intent to Sue EPA for Endangered Species Act and Clean Water Act Violations Related to Idaho Water Quality Standards."
Pham, Q. P., U. Sharma and A. G. Mikos (2006). "Electrospun poly(epsilon-caprolactone) microfiber and multilayer nanofiber/microfiber scaffolds: Characterization of scaffolds and measurement of cellular infiltration." Biomacromolecules **7**(10): 2796-2805.
Pichat, P., C. Guillard, C. Maillard, L. Amalric and J. D'Oliveira (1993). "Titanium dioxide photocatalytic destruction of water aromatic pollutants: intermediates; properties-degradability correlation; effects of inorganic ions and titanium dioxide surface area; comparisons with hydrogen peroxide processes." Photocatalytic Purification and Treatment of Water and Air: 207-223.
Prairie, M. R., L. R. Evans, B. M. Stange and S. L. Martinez (1993). "An Investigation of Tio2 Photocatalysis for the Treatment of Water Contaminated with Metals and Organic-Chemicals." Environmental Science & Technology **27**(9): 1776-1782.
Qamar, M., M. Muneer and D. Bahnemann (2006). "Heterogeneous photocatalysed degradation of two selected pesticide derivatives, triclopyr and daminozid in aqueous suspensions of titanium dioxide." Journal of Environmental Management **80**(2): 99-106.
Rengaraj, S. and X. Z. Li (2006). "Enhanced photocatalytic activity of TiO2 by doping with Ag for degradation of 2,4,6-trichlorophenol in aqueous suspension." Journal of Molecular Catalysis a-Chemical **243**(1): 60-67.
Ryu, Y. J., H. Y. Kim, K. H. Lee, H. C. Park and D. R. Lee (2003). "Transport properties of electrospun nylon 6 nonwoven mats." European Polymer Journal **39**(9): 1883-1889.
Sakata, Y., T. Yamamoto, T. Okazaki, H. Imamura and S. Tsuchiya (1998). "Generation of visible light response on the photocatalyst of a copper ion containing TiO2." Chemistry Letters(12): 1253-1254.
Sakthivel, S., B. Neppolian, M. V. Shankar, B. Arabindoo, M. Palanichamy and V. Murugesan (2003). "Solar photocatalytic degradation of azo dye: comparison of photocatalytic efficiency of ZnO and TiO2." Solar Energy Materials and Solar Cells **77**(1): 65-82.
Salah, M., N. Samy and M. Fadel (2009). "Methylene blue mediated photodynamic therapy for resistant plaque psoriasis." Journal of drugs in dermatology: JDD **8**(1): 42.
Salem, I. A. and M. S. El-Maazawi (2000). "Kinetics and mechanism of color removal of methylene blue with hydrogen peroxide catalyzed by some supported alumina surfaces." Chemosphere **41**(8): 1173-1180.
Saquib, M. and M. Muneer (2003). "TiO(2)-mediated photocatalytic degradation of a triphenylmethane dye (gentian violet), in aqueous suspensions." Dyes and Pigments **56**(1): 37-49.
Sauer, T., G. C. Neto, H. J. Jose and R. F. P. M. Moreira (2002). "Kinetics of photocatalytic degradation of reactive dyes in a TiO2 slurry reactor." Journal of Photochemistry and Photobiology a-Chemistry **149**(1-3): 147-154.
Sayilkan, F., M. Asilturk, S. Sener, S. Erdemoglu, M. Erdemoglu and H. Sayilkan (2007). "Hydrothermal synthesis, characterization and photocatalytic activity of nanosized TiO2 based catalysts for rhodamine B degradation." Turkish Journal of Chemistry **31**(2): 211-221.
Schirmer, R. H., B. Coulibaly, A. Stich, M. Scheiwein, H. Merkle, J. Eubel, K. Becker, H. Becher, O. Muller, T. Zich, W. Schiek and B. Kouyate (2003). "Methylene blue as an antimalarial agent." Redox Report **8**(5): 272-275.
Sclafani, A. and J. M. Herrmann (1996). "Comparison of the photoelectronic and photocatalytic activities of various anatase and rutile forms of titania in pure liquid organic phases and in aqueous solutions." Journal of Physical Chemistry **100**(32): 13655-13661.

Shourong, Z., H. Qingguo, Z. Jun and W. Bingkun (1997). "A study on dye photoremoval in TiO< sub> 2</sub> suspension solution." Journal of Photochemistry and Photobiology A: Chemistry **108**(2): 235-238.
Slimen, H., A. Houas and J. P. Nogier (2011). "Elaboration of stable anatase TiO2 through activated carbon addition with high photocatalytic activity under visible light." Journal of Photochemistry and Photobiology a-Chemistry **221**(1): 13-21.
Son, W. K., J. H. Youk, T. S. Lee and W. H. Park (2004). "The effects of solution properties and polyelectrolyte on electrospinning of ultrafine poly(ethylene oxide) fibers." Polymer **45**(9): 2959-2966.
Song, L. Y., Y. C. Wu and X. F. Lu (2007). "Preparation and Characterization of Doped Nanometer TiO2." Advanced Materials Research **26**: 649-652.
Stankus, J. J., J. J. Guan, K. Fujimoto and W. R. Wagner (2006). "Microintegrating smooth muscle cells into a biodegradable, elastomeric fiber matrix." Biomaterials **27**(5): 735-744.
Stylidi, M., D. I. Kondarides and X. E. Verykios (2004). "Visible light-induced photocatalytic degradation of Acid Orange 7 in aqueous TiO2 suspensions." Applied Catalysis B-Environmental **47**(3): 189-201.
Sukigara, S., M. Gandhi, J. Ayutsede, M. Micklus and F. Ko (2003). "Regeneration of Bombyx mori silk by electrospinning - part 1: processing parameters and geometric properties." Polymer **44**(19): 5721-5727.
Tang, J., Z. Zou, J. Yin and J. Ye (2003). "Photocatalytic degradation of methylene blue on CaIn< sub> 2</sub> O< sub> 4</sub> under visible light irradiation." Chemical physics letters **382**(1): 175-179.
Tang, W. Z., Z. Zhang, H. An, M. O. Quintana and D. F. Torres (1997). "TiO2/UV photodegradation of azo dyes in aqueous solutions." Environmental Technology **18**(1): 1-12.
Tariq, M. A., M. Faisal, M. Muneer and D. Bahnemann (2007). "Photochemical reactions of a few selected pesticide derivatives and other priority organic pollutants in aqueous suspensions of titanium dioxide." Journal of Molecular Catalysis A: Chemical **265**(1): 231-236.
Taylor, G. (1969). "Electrically Driven Jets." Proceedings of the Royal Society of London Series a-Mathematical and Physical Sciences **313**(1515): 453-&.
Teleki, A., N. Bjelobrk and S. E. Pratsinis (2008). "Flame-made Nb- and Cu-doped TiO2 sensors for CO and ethanol." Sensors and Actuators B-Chemical **130**(1): 449-457.
Thiruvenkatachari, R., T. O. Kwon, J. C. Jun, S. Balaji, M. Matheswaran and I. S. Moon (2007). "Application of several advanced oxidation processes for the destruction of terephthalic acid (TPA)." Journal of Hazardous Materials **142**(1-2): 308-314.
Tseng, I. H., J. C. S. Wu and H. Y. Chou (2004). "Effects of sol-gel procedures on the photocatalysis of Cu/TiO2 in CO2 photoreduction." Journal of Catalysis **221**(2): 432-440.
Tseng, T. K., Y. S. Lin, Y. J. Chen and H. Chu (2010). "A Review of Photocatalysts Prepared by Sol-Gel Method for VOCs Removal." International Journal of Molecular Sciences **11**(6): 2336-2361.
Ustinovich, E. A., D. G. Shchukin and D. V. Sviridov (2005). "Heterogeneous photocatalysis in titania-stabilized perfluorocarbon-in-water emulsions: Urea photosynthesis and chloroform photodegradation." Journal of Photochemistry and Photobiology a-Chemistry **175**(2-3): 249-252.
Wang, C. C. and J. Y. Ying (1999). "Sol-gel synthesis and hydrothermal processing of anatase and rutile titania nanocrystals." Chemistry of Materials **11**(11): 3113-3120.
Wannatong, L., A. Sirivat and P. Supaphol (2004). "Effects of solvents on electrospun polymeric fibers: preliminary study on polystyrene." Polymer International **53**(11): 1851-1859.
Wu, S. D., Y. Q. Zhu, C. Li and Y. L. Wei (2011). "A Novel CuO-TiO2 Composite Photocatalyst and its Degradation of Methyl Orange under UV Irradiation." Advanced Materials Research **295**: 1129-1132.
Xiao, Q., J. Zhang, C. Xiao, Z. Si and X. Tan (2008). "Solar photocatalytic degradation of methylene blue in carbon-doped TiO2 nanoparticles suspension." Solar Energy **82**(8): 706-713.
Xu, N., Z. Shi, Y. Fan, J. Dong, J. Shi and M. Z. C. Hu (1999). "Effects of Particle Size of TiO2 on Photocatalytic Degradation of Methylene Blue in Aqueous Suspensions." Industrial & Engineering Chemistry Research **38**(2): 373-379.

Xu, Y. H., D. H. Liang, M. L. Liu and D. Z. Liu (2008). "Preparation and characterization of Cu(2)O-TiO(2): Efficient photocatalytic degradation of methylene blue." Materials Research Bulletin **43**(12): 3474-3482.
Yamashita, H., M. Takeuchi and M. Anpo (2004). "Visible-Light-Sensitive Photocatalysts." Encyclopedia of nanoscience and nanotechnology **10**(1): 639-654.
Yan, X., T. Ohno, K. Nishijima, R. Abe and B. Ohtani (2006). "Is methylene blue an appropriate substrate for a photocatalytic activity test? A study with visible-light responsive titania." Chemical Physics Letters **429**(4–6): 606-610.
Yarin, A. L., S. Koombhongse and D. H. Reneker (2001). "Bending instability in electrospinning of nanofibers." Journal of Applied Physics **89**(5): 3018-3026.
Yordem, O. S., M. Papila and Y. Z. Menceloglu (2008). "Effects of electrospinning parameters on polyacrylonitrile nanofiber diameter: An investigation by response surface methodology." Materials & Design **29**(1): 34-44.
Yuan, X. Y., Y. Y. Zhang, C. H. Dong and J. Sheng (2004). "Morphology of ultrafine polysulfone fibers prepared by electrospinning." Polymer International **53**(11): 1704-1710.
Zeleny, J. (1914). "The electrical discharge from liquid points, and a hydrostatic method of measuring the electric intensity at their surfaces." Physical Review **3**(2): 69-91.
Zendehdel, M., A. Barati, H. Alikhani and A. Hekmat (2010). "Removal of Methylene Blue Dye from Wastewater by Adsorption onto Semi-Inpenetrating Polymer Network Hydrogels Composed of Acrylamide and Acrylic Acid Copolymer and Polyvinyl Alcohol." Iranian Journal of Environmental Health Science & Engineering **7**(5): 423-428.
Zhang, C. X., X. Y. Yuan, L. L. Wu, Y. Han and J. Sheng (2005). "Study on morphology of electrospun poly(vinyl alcohol) mats." European Polymer Journal **41**(3): 423-432.
Zong, X., K. Kim, D. Fang, S. Ran, B. S. Hsiao and B. Chu (2002). "Structure and process relationship of electrospun bioabsorbable nanofiber membranes." Polymer **43**(16): 4403-4412.
Zong, X. H., K. Kim, D. F. Fang, S. F. Ran, B. S. Hsiao and B. Chu (2002). "Structure and process relationship of electrospun bioabsorbable nanofiber membranes." Polymer **43**(16): 4403-4412.